Molecular Neurobiology (2019) 56:1310–1329
https://doi.org/10.1007/s12035-018-1160-3

Tissue-Specific Upregulation of *Drosophila* Insulin Receptor (InR) Mitigates Poly(Q)-Mediated Neurotoxicity by Restoration of Cellular Transcription Machinery

Kritika Raj[1] · Surajit Sarkar[1]

Received: 24 July 2017 / Accepted: 29 May 2018 / Published online: 7 June 2018

Abstract

Polyglutamine [poly(Q)] disorders are a class of trinucleotide repeat expansion neurodegenerative disorders which are dominantly inherited and progressively acquired with age. This group of disorders entail the characteristic formation of protein aggregates leading to widespread loss of neurons in different regions of the brain. SCA3 and HD, the two most commonly occurring types of poly(Q) disorders were examined in the present study. With the aim of elucidating novel genetic modifiers of poly(Q) disorders, the *Drosophila* insulin receptor (InR) was identified as a potential suppressor of poly(Q)-induced neurotoxicity and degeneration. We demonstrate for the first time that targeted upregulation of InR could effectively mitigate poly(Q)-mediated neurodegeneration in fly models. A significant reduction in poly(Q)-mediated cellular stress and apoptosis was noted upon InR overexpression in poly(Q) background. We further reveal that targeted upregulation of InR causes a substantial reduction in poly(Q) aggregate formation with the residual inclusion bodies localised to the cytoplasm. We also demonstrate that InR achieves suppression of poly(Q) toxicity by replenishing the cellular pool of CREB binding protein and improving the histone acetylation status of the cell. This leads to restoration of the cellular transcriptional machinery which is otherwise severely compromised in poly(Q) disease conditions. Interestingly, there also appeared a possibility of autophagy-mediated rescue of poly(Q) phenotype due to upregulation of InR. Therefore, our study strongly suggests that modulation of the insulin signalling pathway could be an effective therapeutic intervention against poly(Q) disorders.

Keywords *Drosophila* · Poly(Q) · InR · Neurodegeneration

Introduction

Polyglutamine [poly(Q)] disorders represent a group of dominantly inherited age onset devastating neurological illnesses which are characterised by progressive course of a common pathogenic mechanism. Manifestation of disease phenotypes marks the crossing of the threshold repeat length of the poly(CAG) expansion within affected proteins. As a result, each of the nine different poly(Q) disorders known shows discrete pattern of neuronal degeneration but overlapping phenotypes such as late onset, formation of protein aggregates and gradual degeneration of affected neurons [1]. Some of the commonly found poly(Q) disorders include Huntington's disease (HD), Spinocerebellar ataxia type 1, 2, 3, 6, 7, and 17, Spinal and bulbar muscular atrophy (SBMA) and Dentatorubral-pallidoluysian atrophy (DRPLA) [2]. Though the affected protein in each case harbours an inherent poly(CAG) tract, however, each of these proteins exhibits predisposition towards genetic anticipation [3]. The extra glutamine residues acquired as a result of various genetic mutations renders the protein to be pathogenic in nature through a variety of ways, including aberrant folding and degradation pathways, altered subcellular localization, and anomalous interactions with other cellular proteins [4]. Extended poly(Q) containing mutated proteins often aggregate together to form nuclear inclusion bodies [5] which leads to neuronal dysfunction and eventually, neuronal death.

Spinocerebellar ataxia type 3 (SCA3) and Huntington's disease (HD) represent the two most commonly occurring forms of poly(Q) disorders worldwide. The affected protein in case of

Electronic supplementary material The online version of this article (https://doi.org/10.1007/s12035-018-1160-3) contains supplementary material, which is available to authorized users.

✉ Surajit Sarkar
sarkar@south.du.ac.in

[1] Department of Genetics, University of Delhi South Campus, Benito Juarez Road, Dhaula Kuan, New Delhi 110021, India

SCA3 is the deubiquitinating enzyme ataxin-3 encoded by the *ATXN3* gene (cytogenetic position 14q24.3–32), and in case of HD is the huntingtin protein involved in nerve cell function and encoded by the *htt* gene (cytogenetic position 4p16.3). As discussed above, an elongated CAG tract in the coding sequence of these genes causes mis-folding of the protein and subsequent cleavage by active caspases into fragments which are further altered to form microscopically visible aggregates called inclusion bodies (IBs) [6]. The inclusion body formation is a hallmark and the most common characteristic feature of all the poly(Q) diseases [7]. Such inclusion bodies sequester other proteins harbouring short non-pathogenic glutamine repeats by homotypic glutamate interactions and thus, deplete the cellular pool of essential proteins further aggravating cellular toxicity [8]. The proteins most commonly held inside IBs include key molecular chaperones like HSP 70 and HSP 90, ubiquitin-proteasomal components, crucial transcription factors like TBP-associated factor (TAFII130), specificity factor (SP1), CREB binding protein (CBP), as well as important initiator and effector caspases [9]. This results in impaired signalling and transcription in the cell leading to neuronal toxicity and degeneration [10]. Furthermore, it has also been reported that pathways essential for maintenance of proper cellular homeostasis, such as autophagy and apoptosis, are altered under poly(Q)-induced disease conditions which also contributes to aggravated neurotoxicity [11, 12].

The insulin-like growth factor receptor (IGF-R) signalling pathway is an established regulator of growth and energy metabolism in both vertebrates and invertebrates. It is, in fact, the major pathway known to play role in growth and development of cells and tissues, including neurons [13]. In addition to promoting cell differentiation and proliferation, the IGF-R signalling pathway also plays a major role in preventing cell death by activating various anti-apoptotic triggers [14, 15]. Interestingly, several studies have demonstrated reduced levels of IGF-R mRNA as well as protein in neurodegenerative disorders pointing towards a probable role of IGF-R signalling in their pathogenesis [16, 17]. In this cascade, *myc* functions as a downstream effector of the IGF-R signalling pathway, playing an important role in growth and development of neuronal tissues [18]. Since a previous study from the lab has demonstrated that dMyc (*Drosophila* homologue of the human *c-myc* proto-oncogene) can act as a potent suppressor of poly(Q)-induced neurotoxicity [19], we wanted to further examine whether any other player of this pathway also harbours poly(Q) modifier potential so that it can be exploited in a combinatorial drug approach against poly(Q) disorders in the near future.

Based on extensive genetic screening and subsequent preliminary analysis, we identified the *Drosophila insulin-like growth factor receptor* (*inr*) gene as a potent modifier of poly(Q)-induced neurotoxicity. We report for the first time that targeted upregulation of the insulin signalling pathway by overexpressing full length InR (*Drosophila* homologue of human insulin-like growth factor 1 receptor) can significantly suppress poly(Q)-induced neurodegeneration and the associated phenotypes with reduced formation of inclusion bodies. Moreover, upregulation of InR was shown to alleviate poly(Q)-induced cellular stress and apoptosis as well as enhance autophagic events in an attempt to rescue the disease condition. We further articulate that the observed rescue is largely due to enhanced expression of CBP and histone modifications pointing towards chromatin-remodelling-mediated global transcriptional improvement and restored gene expression. This is the first report which successfully establishes the potential of InR to induce chromatin remodelling in poly(Q) disease background. Thus, the IGF-R signalling pathway appeared as a promising candidate to review in context of neurodegenerative disease models.

Materials and Methods

Drosophila Fly Stocks

The *Drosophila* stocks used in the experiments were reared in cornmeal/agar/yeast media at 24 ± 1 °C. *Oregon* R^+ was used as wild type wherever indicated. The transgenic lines w;*UAS-SCA3trQ78(S)/CyO;+/+* [20], w;+/+;*UAS-SCA3trQ78(M)/UAS-SCA3trQ78(M)* [21], w;*GMR-GAL4/GMR-GAL4;+/+* [22], w;*Elav-GAL4/CyO;+/+* [23], w;*201Y-GAL4/201Y-GAL4;+/+* [24], w;*UAS-InR.Exel/UAS-InR.Exel;+/+*, *w;+/+;UAS-InR-RNAi/UAS-InR-RNAi*, w;*UAS-DIAP1/UAS-DIAP1;+/+*, w;*UAS-GFP/UAS-GFP;+/+*; *w;+/+;UAS-GFP/UAS-GFP* (Bloomington Stock Centre, Indiana, USA), *w;+/+;UAS-InR-CFP/UAS-InR-CFP* [25], *w;UAS-HttQ15-mRFP/UAS-HttQ15-mRFP;+/+*, w;+/+;*UAS-HttQ138-mRFP/UAS-HttQ138-mRFP* [26], w;*UAS-Htt93Q/UAS-Htt93Q;+/+* [27], w;*UAS-dCBPΔBHQ/UAS-dCBPΔBHQ;+/+*, *w;+/+;UAS-dCBP-RNAi/UAS-dCBP-RNAi* [28] were either procured from Bloomington *Drosophila* stock centre, IN, USA, or obtained from various laboratories as referred above.

Morphological Examination and Pseudopupil Analysis of Adult Eye

Bright field and RFP fluorescence image acquisition of *Drosophila* adult eye was carried out as described earlier [19]. For scanning electron microscopy (SEM), adult heads of desired genotype were decapitated in 1× PBS and fixed in 2% paraformaldehyde + 2.5% glutaraldehyde at 4 °C for overnight. The tissues were dehydrated in acetone and critically-dried using Leica EM CPD300 system. The heads were mounted on studs under stereo zoom binocular microscope and coated with ~ 30-nm gold. Images were captured using a

JEOL JSM-6610LV scanning electron microscope. For pseudopupil analysis, which allows observation of photoreceptors in the adult eye, heads were decapitated and processed as described earlier [19].

Phototaxis, Survival and Longevity Assay

Phototaxis assay was carried out using a Y maze design as described earlier [19]. For the survivability test, the number of flies eclosing as adults from mature pupae was recorded and statistical analysis was performed according to procedures described earlier [19]. For evaluating the longevity of flies of desired genotype, procedures as described earlier [29] were carried out and average life expectancy of the flies was calculated.

Histology and Immunohistochemistry

Histology of *Drosophila* adult eye and immunohistochemistry of third instar larval eye disc/adult head were carried out as described earlier [19]. The primary antibodies used were anti-InR (1:1000, gift from Prof. Dr. Ernst Hafen), anti-Fasciclin II (1:100; ID4, DSHB, USA), anti-cleaved caspase-3 (1:1000, D175, Cell Signaling Technology, USA), anti-HSP70 (1:200, 5A5, Thermo Scientific, USA), anti-LC3 A/B (1:100, ab128025, Abcam, UK), anti-HA (1:1000; Y11, Santa Cruz Biotechnology, USA), anti-dCBP (1:500) [30], anti-Histone H3 (acetylK9) (1:1000, ab12179, Abcam, UK) and anti-Histone H3 (dimethylK9) (1:200, ab1220, Abcam, UK). The secondary probes were Alexa 488 goat anti-rabbit (A11008), Alexa 488 goat anti-mouse (A10001), Alexa-488 goat anti-guinea pig (A11073), Cy3 goat anti-rabbit (A10520), Cy3 goat anti-mouse (A10521). For staining with TRITC-Phalloidin, fixed eye tissues of 55-h-old pupae were incubated in 1:200 dilution of TRITC-Phalloidin (P1951, Sigma-Aldrich, USA) for 1 h at 25 °C. In some cases, tissues were counterstained with DAPI (5 μg/ml, Roche Diagnostics, GmbH, Germany) and thereafter mounted in prolong gold antifade mounting reagent (Molecular probes, USA). The images were captured either by Olympus BX51 or BX53 fluorescence microscope using appropriate filters or Leica TCS SP5 II confocal microscope. Equal numbers of confocal optical section images were taken while constructing comparative merge images with Leica application suite advanced fluorescence software. The pictures were assembled using Adobe Photoshop CS5 software.

Lyso Tracker Red and Acridine Orange Staining

Lyso Tracker Red DND-99 (L7528, Molecular Probes, USA) is a red fluorescent dye used for labelling and tracking acidic organelles in live cells whereas Acridine orange (A1301, Molecular Probes, USA) is a vital dye that preferentially binds to fragmented DNA and therefore labels apoptotic cells in the given tissue. Third instar larval eye disc tissues (maximum of 5 discs each time) were dissected in 1× PBS and incubated with Lyso Tracker Red DND-99 (1:1000) or acridine orange (0.2 mg/ml) for 5 min. The tissues were immediately washed in PBS twice for 2 min each after which the buffer was changed once more and the tissues were immediately visualised under Olympus BX51 flourescence microscope using appropriate filters.

Bromouridine Staining and TUNEL Assay

For bromouridine incorporation assay, third instar larval eye discs were dissected in 1× PBS and incubated at room temperature in 10 μM bromouridine (BrdU) (Sigma, USA) diluted in Schneider's medium (Sigma, USA). Subsequently, tissue fixation, DNA denaturation and neutralisation and antibody treatment was carried out according to procedures described earlier [29].

Terminal deoxynucleotidyl transferase dUTP nick-end labelling (TUNEL) assay was performed to detect apoptotic cell death in third instar larval eye discs as well as in paraffin embedded adult head sections of 2-day old adult flies as per manufacturer's protocol (DeadEnd™ Flourometric TUNEL System, Promega, USA). The images were captured using Leica TCS SP5 II confocal microscope and TUNEL-positive cells were quantified and plotted using MS Excel 2010.

Protein Extraction and Western Blotting

Protein extraction and western blotting was carried out from 2-day-old adult flies following protocols described earlier [29]. The primary antibodies used for probing protein lysates were anti-LC3 A/B (1:500, ab128025, Abcam, UK), anti-HA (1:1000; Y11, Santa Cruz Biotechnology, USA), anti-histone H3 acetylK9 (1:1000, ab12179, Abcam, UK) and anti-β-tubulin (1:1000, E7, DSHB, USA). The secondary probes used to detect primary antibodies were conjugated to horseradish peroxidase (HRP) (1:2000, Merck, USA) which reacts with the ECL substrate to generate a signal that was detected using the FUJIFILM LAS-4000 image reader.

Statistical Analysis

Statistical analysis was performed using the student *t* test, and error bars on figures represent the mean ± SD. Differences were considered to be significant at $*p$ value < 0.05, $**p$ value < 0.01 and $***p$ value < 0.001.

Results

Targeted Overexpression of InR Suppresses Poly(Q)-Induced Morphological Deficits in *Drosophila* Model of Human SCA3

In order to evaluate the effect of altered expression of InR in poly(Q) disorders, we utilised a *Drosophila* model of human SCA3 which expresses an HA-tagged truncated form of ataxin-3 protein containing 78 CAG repeats [*SCA3trQ78(S)*] in tissue-specific manner using the yeast upstream activating sequence (UAS)-GAL4 system [20, 31]. It has been demonstrated earlier that targeted expression of *SCA3trQ78(S)* in the *Drosophila* eye using the glass multiple receptor (GMR) driver [22] (henceforth referred as *UAS-SCA3trQ78(S)-GMR-GAL4*) results in severe degeneration of the eye [21, 32]. In agreement with earlier reports, compared to control *GMR-GAL4/+* flies which display normal eye morphology (Fig. 1a), *UAS-SCA3trQ78(S)-GMR-GAL4* flies exhibited acute degeneration of the eye surface which was prominent even on the first day of eclosion (Fig. 1b). The morphological defects manifested in the form of loss of eye pigmentation, reduced eye size, disrupted ommatidial arrangement and disoriented bristle lattice pattern. Moreover, in many of the adult eyes, formation of black necrotic lesions over the surface of the eye was noted which is indicative of severely degenerated tissue and cell death (Fig. 1b). For determining the rescue potential of InR against poly(Q)-induced toxicity, this particular disease line was crossed with *UAS-InR* line which expresses wild type *Drosophila* insulin receptor under *UAS* control. Upon coexpression of the *UAS-InR* transgene in the *Drosophila* eye along with *UAS-SCA3trQ78(S)* (henceforth referred as *UAS-SCA3trQ78(S)-GMR-GAL4/UAS-InR*), a significant improvement in the eye morphology was noted (Fig. 1c). Eye pigmentation was restored to a considerable extent, eye size was augmented, the ommatidial and bristle lattice appeared uniform and the necrotic patches were not observed in the progenies collected ($n \geq 500$). Interestingly, RNAi-mediated downregulation of InR in disease background, on the other hand, resulted in exaggerated disease toxicity as large necrotic patches were evident on the eye surface with complete loss of pigmentation and ommatidial structure (Fig. 1d). Most importantly, upon chasing the rescue event with age, it was found that InR was able to sustainably suppress poly(Q)-induced degeneration throughout the lifespan of the fly (Fig. S1 c–l). The eye pigments persisted even 20 days post eclosion and there was no appearance of necrotic patches (Fig. S1) as opposed to diseased flies that exhibited large patches of necrotic death and severe degeneration with age (Fig. S1 b–k). The control *GMR-GAL4/+* flies did not show any detectable phenotypic changes in the eye with age (Fig. S1 a–j).

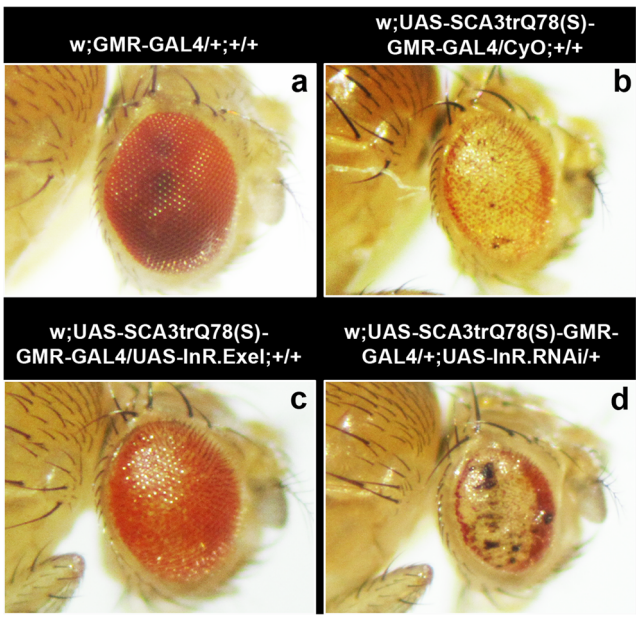

Fig. 1 *GMR-GAL4* driven overexpression of InR suppresses poly(Q)-induced neurodegeneration in the *Drosophila* eye. **a**–**d** Bright field images of the external surface of the adult eye. **a** Eye from *w;GMR-GAL4/+;+/+* control fly. **b** Degenerated eye with reduced size, loss of pigmentation and appearance of black necrotic patches following expression of *SCA3trQ78(S)*. **c** Restored cellular degeneration and roughening of eye surface following coexpression of InR. **d** Exaggerated poly(Q)-induced neurotoxicity and appearance of large necrotic patches upon RNAi mediated downregulation of InR in poly(Q) background

In order to exclude the possibility of any change in phenotype due to insertion of two UAS transgenes in the genome, the effect of the expression of *UAS-GFP* transgene on the disease phenotype was observed. Coexpression of *UAS-GFP* in *SCA3trQ78(S)* background does not result in any phenotypic change (Fig. S2a) and thus suggests that the rescue event was indeed mediated by overexpression of InR. Further, the modifier potency of InR was found to be superior in comparison to other established modifier of poly(Q) disorders such as DIAP1 (*Drosophila* inhibitor of apoptosis) (Fig. S2b) [33, 34]. It was also noted that overexpression or downregulation of InR itself did not cause any phenotypic changes in the eye except insignificant alterations in the eye size (Fig. S2c, d) which were expected owing to the growth promoting properties of InR. An additional control was employed at this stage to substantiate that the rescue event is indeed due to specific modifier effects of InR on poly(Q) and that its upregulation does not alter the expression of a neutral transgene. For this, the expression level of *GMR-GAL4* driven *UAS-GFP* transgene was analysed in different genotypes, and no significant change was noted in the level of GFP expression across all the four genotypes examined (Fig. S3). This suggests that GAL4-mediated coexpression of *UAS-InR* does not make any impact on the expression level of an additional independent transgene.

Subsequent to above, scanning electron microscopy (SEM) was carried out in order to study the external surface of the eye in greater details. The control *GMR-GAL4/+* eye (2 days old) revealed a regular arrangement of ommatidia and properly oriented bristle lattice (Fig. 2a, a'); however, eyes from *UAS-SCA3trQ78(S)-GMR-GAL4* adults were severely deformed and ommatidia tended to collapse upon critical drying due to lack of underlying tissue mass (Fig. 2b). The bristles were found to be highly disoriented when observed at higher magnification (Fig. 2b'). Upregulation of InR displayed significant improvement in external eye morphology with appropriately arranged ommatidia and bristles (Fig. 2c, c'). In order to examine the comparative internal architecture of the adult eyes, 15-μm thick horizontal sections of the eye were prepared and stained with 0.01% Toluidine Blue stain. It was observed that in comparison to the control *GMR-GAL4/+* tissues which showed distinctly arranged lamina, retina and ommatidial facet (Fig. 2d), eye-specific expression of *UAS-SCA3trQ78(S)* transgene resulted in severe degeneration of the internal eye tissues with lack of majority of cellular mass in the retinal region (Fig. 2e). Coexpression of InR in *SCA3trQ78(S)* expressing tissues was found to significantly improve the internal eye structure and also suppress retinal degeneration (Fig. 2f).

Another cellular feature that was used to determine the rescue proficiency of InR was F-actin organisation. Since poly(Q)-mediated defects start manifesting at the pupal stage [20], morphological studies were also performed on the developing pupal eyes. The *Drosophila* compound eye is made up of around 600 regularly arranged units called ommatidia, each of which is composed of 20 cells—1 corneal cell, 2 primary cells, 3 secondary cells, 3 tertiary cells, 3 bristles and 8 photoreceptor cells whose rhabdomeres project towards the centre of the ommatidium. Since, the 8th photoreceptor cell lies just below the 7th, therefore, all the photoreceptors cannot be visualised at the same focal plane. For F-actin analysis, pupal eye discs were stained with Phalloidin which is a marker of F-actin and effectively stains the cellular boundaries as well as photoreceptor pigments present at the centre of each ommatidia. Pupal eyes from *GMR-GAL4/+* displayed proper hexagonal array of ommatidia and the seven rhabdomeres present within were found to be arranged in a typical trapezoid arrangement (Fig. 2g) whereas expression of *UAS-SCA3trQ78(S)* led to unstructured assembly and altered arrangement of ommatidia (Fig. 2h). Interestingly, coexpression of InR restored the ommatidial architecture to a significant extent and also substantially reinstated the rhabdomere structures (Fig. 2i).

In order to ascertain that the rescue event observed in the eye was indeed achieved by overexpression of InR in the target tissues, third instar larval eye discs were stained with antibody specific to *Drosophila* InR. Compared to the control *GMR-GAL4/+* eye discs which displayed a basal level of InR

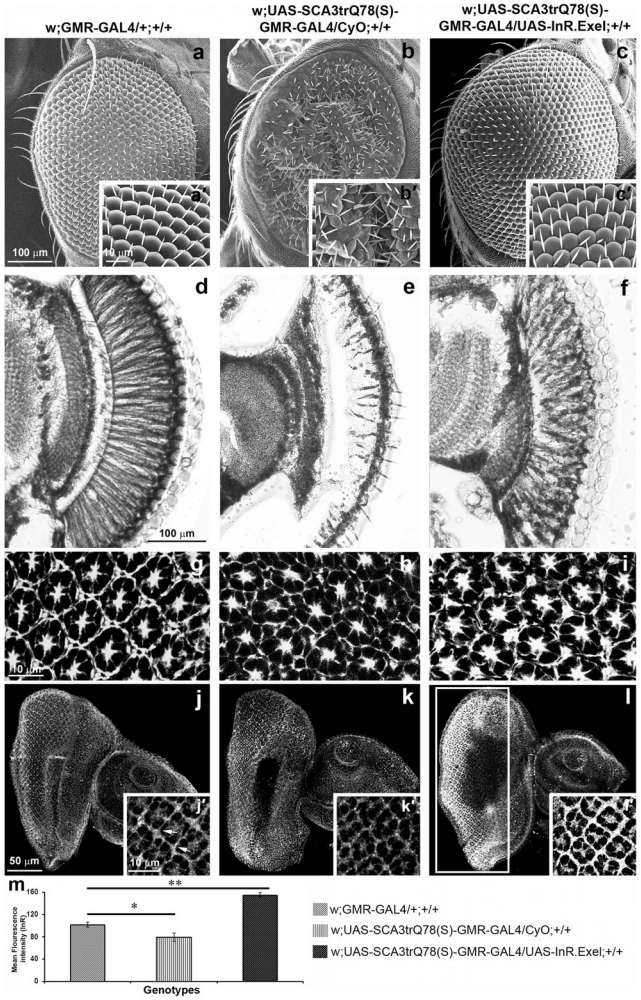

Fig. 2 Upregulation of InR improves external and internal cellular architectures which are disrupted upon eye-specific expression of poly(Q) in *Drosophila*. **a**–**c**, **a′**–**c′** Scanning electron microscopy (SEM) images of adult *Drosophila* eye. **a**, **a′** SEM image of control *w;GMR-GAL4/+;+/+* fly. **b**, **b'** Degenerated eye and disrupted ommatidial arrangement in poly(Q) expressing flies. **c**, **c′** Coexpression of InR prevented poly(Q)-induced deterioration of the eye and restored ommatidial architecture as well as bristle lattice. **d**–**f** Toluidine blue-stained horizontal sections of eye retina. **d** *w;GMR-GAL4/+;+/+* control. **e** Degenerated retinal mass due to expression of *SCA3trQ78(S)*. **f** Coexpression of InR suppressed retinal degeneration and restored internal eye architecture. **g**–**i** Confocal images of pupal eye stained with TRITC-Phalloidin. **g** Control *w;GMR-GAL4/+;+/+* pupal eye showed regular array of hexagonally shaped ommatidia with a cluster of seven photoreceptors at the centre of each unit. **h** distorted ommatidial arrangement and abnormal distribution of photoreceptors upon expression of *SCA3trQ78(S)* transgene. **i** Coexpression of InR improves rhabdomere arrangement and morphology. **j**–**l, j′**–**l′** Confocal images of eye discs stained with anti-InR. **j**, **j′** Basal level expression of InR in control eye discs. Arrows in **j′** show membrane-specific expression of InR. **k**, **k′** Reduced InR expression in SCA3 expressing eye discs. **l**, **l′** Significantly enhanced expression of InR in the region posterior to the morphogenetic furrow following coexpression of *InR* transgene in disease background. InR expression was found to be evidently membrane-specific. **m** Histogram representing the relative fluorescence intensities InR staining. (*Scale bars*: **a**–**c**, **e**–**f** = 100 μm; **a′**–**c′**, **g**–**i**, **j′**–**l'** = 10 μm; **j**–**l** = 50 μm; * = $P < 0.05$; ** = $P < 0.01$)

expression confined to the cell boundaries (Fig. 2j'), eye-specific expression of *SCA3trQ78(S)* resulted in reduced expression of InR which may be attributed to compromised cellular signalling in diseased condition (Fig. 2k, k'; also see m) [35]. In contrast, coexpression of *UAS-InR* transgene in *SCA3trQ78(S)* expressing tissues resulted in robust expression of InR confined to the region posterior to the morphogenetic furrow (region containing differentiated neuronal cells) (Fig. 2l, m). When observed under higher magnification, the cell boundaries displayed distinctly elevated expression of InR which is characteristic of a receptor protein as it localises to the cellular membrane (Fig. 2l'). Above observations confirm the tissue-specific elevated level of InR in the rescue flies.

Similar expression results were obtained on using a different InR stock which expresses a C-terminally Cyan Flourescent Protein (CFP) tagged *Drosophila* insulin receptor, *UAS-InR-CFP* [25]. Whereas *GMR-GAL4/+* and *UAS-SCA3trQ78(S)-GMR-GAL4/+* eye discs exhibited absence of any CFP expression (Fig. S4a, b), InR was shown to be beautifully localised to the cell membranes of differentiated cells present below the morphogenetic furrow in *UAS-SCA3trQ78(S)-GMR-GAL4/+;UAS-InR-CFP/+* eye discs (Fig. S4c). On analysing the same flies as adults, it was found that the InR-CFP expressing flies also exhibited suppression of the morphological defects associated with poly(Q) (Fig. S4f). Above observations suggest that InR-CFP allele also possesses the capability of mitigating poly(Q)-induced neurotoxicity, though the extent of rescue was slightly less as compared to InR.Exel (compare Fig. 1c with S4f). Moreover, it was reaffirmed that the rescue event was indeed due to expression of InR-CFP as fluorescence imaging of the adult heads revealed strong CFP expression in the eye region of the *UAS-SCA3trQ78(S)-GMR-GAL4/+;UAS-InR-CFP/+* flies (Fig. S4i) in comparison to lack of any CFP expression in the control and diseased flies (Fig. S4g, h). Taken together, above results unambiguously establish that tissue-specific upregulation of InR suppresses human poly(Q)-induced neurodegenerative phenotypes without affecting cellular dynamics.

Upregulation of InR Alleviates Poly(Q)-Mediated Degeneration of Brain Tissues and Confers Functional Rescue

In order to further substantiate the rescue efficacy of InR, we used a less toxic line of SCA3 transgene—*UAS-SCA3trQ78(M)* [21]. Interestingly, compared to the control *GMR-GAL4/+* flies, eye-specific expression of *UAS-SCA3trQ78(M)* did not exhibit any visible external morphological deficits (compare Fig. 3a with Fig. 3b). However, deep pseudopupil analysis in 5-day-old flies revealed substantial degeneration of photoreceptor cells (Fig. 3e) compared to seven photoreceptors in each ommatidium of *GMR-GAL4/+* flies (Fig. 3d). An average of only one or two photoreceptor(s) was

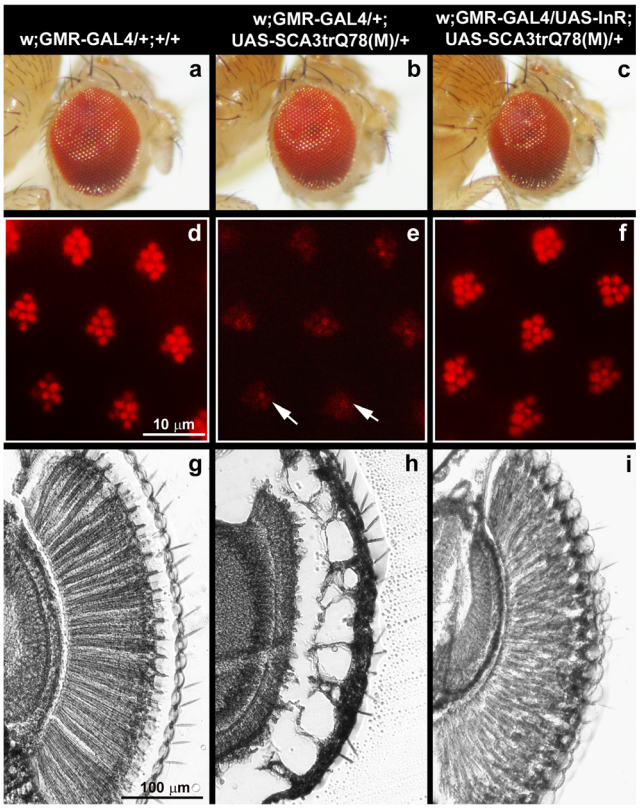

Fig. 3 Targeted overexpression of InR restores functional photoreceptors and improves internal eye morphology in weak form of SCA3. **a**–**c** Bright field pictures of adult eye. *GMR-GAL4*-driven expression of *SCA3trQ78(M)* does not produce any visible phenotypes in external eye morphology nor does the coexpression of InR. **d**–**f** Deep pseudopupil images of adult eye. **d** Seven photoreceptors are observed in controls. **e** Expression of *SCA3trQ78(M)* led to degeneration of photoreceptors (arrows). **f** Coexpression of InR restored the number of photoreceptors. **g**–**i** Toluidine blue stained horizontal sections of eye retina. **g** *w;GMR-GAL4/+;+/+* control. **h** Retinal tissue is degraded due to expression of *SCA3trQ78(M)* transgene. **i** Coexpression of InR reinstated retinal architecture to a significant extent. (*Scale bars*: **d**–**f** = 10 μm; **g**–**i** = 100 μm)

evident in each ommatidium (arrows in Fig. 3e) of flies expressing *SCA3trQ78(M)*. Coexpression of InR in *SCA3trQ78(M)* expressing tissues restricted the degeneration of the photoreceptor cells and each ommatidium displayed an average of 5–6 photoreceptors (Fig. 3f). Subsequently, the integrity of the internal retinal tissues of these flies was studied by staining the horizontal eye sections with toluidine blue. Compared to *GMR-GAL4/+* (Fig. 3g), adult eyes from *GMR-GAL4/+;UAS-SCA3trQ78(M)/+* flies exhibited widespread loss of internal retinal mass with little residual tissue visible under the external eye surface (Fig. 3h). Interestingly, targeted coexpression of InR impeded disease pathogenesis and the density of retinal mass was restored to as good as the control tissues (Fig. 3i).

In order to examine whether the InR mediated restored cellular architecture also led to restoration of the poly(Q)-mediated functional impairments, phototaxis assay was

performed with 5-day-old adult flies of different genotypes. The Y-maze phototaxis assay is based on the rationale that flies with normal vision will inevitably choose the illuminated arm of the Y-maze whereas flies with compromised vision will randomly choose either the illuminated or the dark arm of the Y-maze [36]. In *GMR-GAL4/+* population, around 96% of flies were found to move towards the illuminated arm of the Y-maze (Fig. 4a; $n = 274$). Eye-specific expression of *SCA3trQ78(M)* severely affected the vision and almost equal percentage of flies moved into the light and the dark arm of the Y-maze (Fig. 4a; $n = 235$). Interestingly, a significant increase in positive phototaxis was noted due to eye-specific upregulation of InR in *SCA3trQ78(M)* expressing flies as around 80% flies migrated to the light arm (Fig. 4a; $n = 425$). Above observation clearly demonstrates that enhanced expression of InR not only mitigates cellular degeneration, but also restores the poly(Q)-mediated functional impairments.

In view of the fact that poly(Q) disorders primarily affect the central nervous system (CNS), it was imperative to examine the modifier capacity of InR when the poly(Q) protein was expressed in a specific part of the brain or in pan neuronal manner. For this, two independent GAL4 lines were utilised—*Elav-GAL4* and *201Y-GAL4*. The former expresses pan neuronally in the central and peripheral nervous systems whereas the latter expresses exclusively in the Kenyon cells (a type of neuronal subpopulation) of the mushroom body of the *Drosophila* brain [23, 24]. Since cognitive functions are particularly affected in human and animal models suffering from poly(Q) disorders [37] and the *Drosophila* mushroom body is the functional homologue of hippocampus of higher mammals involved in controlling cognitive functions such as olfactory learning, associative memory as well as courtship, it was essential to study the effect of expressing the mutated SCA3 protein in the mushroom body and examining the

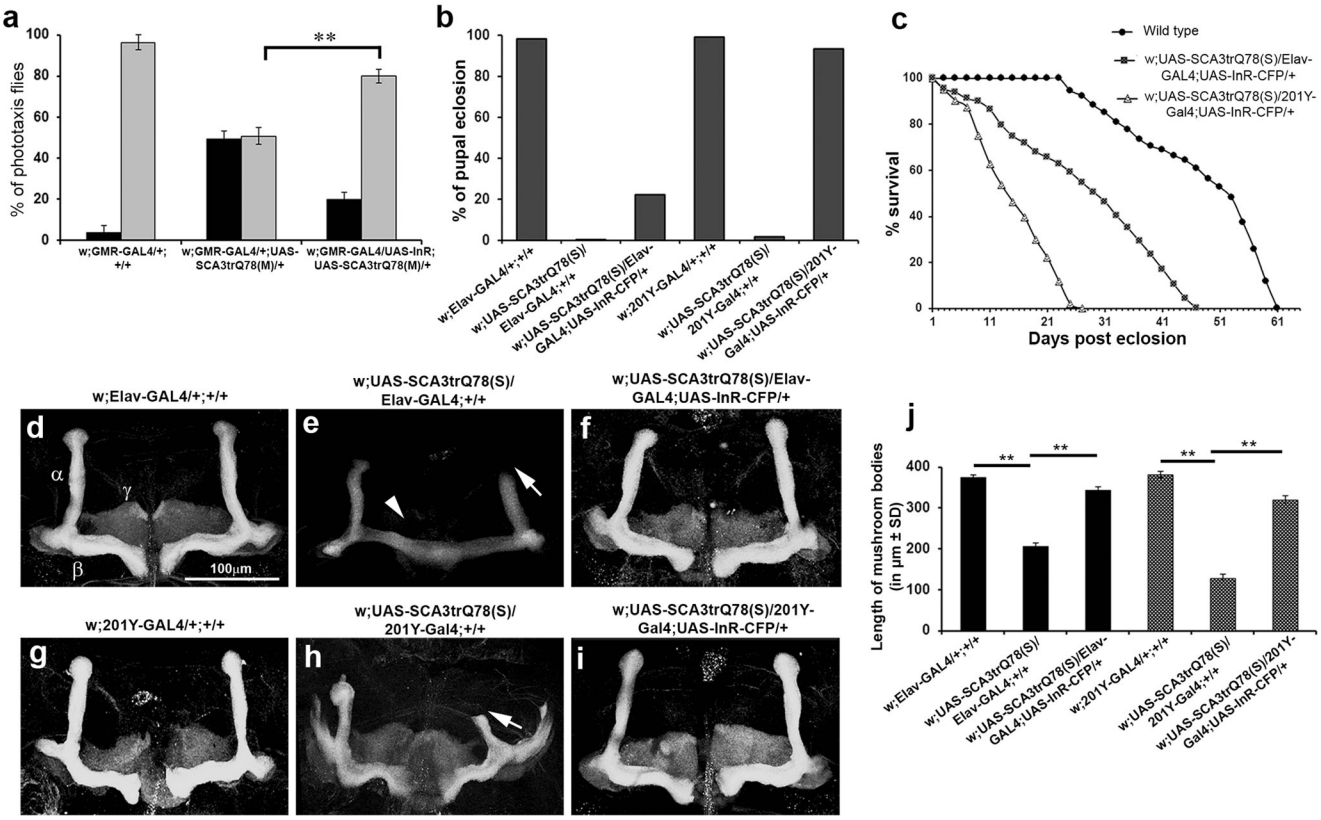

Fig. 4 Upregulation of InR restores functional vision and prevents poly(Q)-mediated brain degeneration. **a** Poly(Q)-induced impairment of vision that is alleviated by coexpression of InR. Bars in histogram represent mean value (± SD) of either positively or negatively phototaxis flies. **b** Pupal lethality induced by expression of *SCA3trQ78(S)* either pan neuronally or in mushroom body tissues is rescued by coexpression of InR-CFP. **c** Longevity analysis of flies expressing InR-CFP in poly(Q) disease background in pan neuronal tissues or mushroom body in comparison to wild type flies. **d**–**i** Confocal images of adult brain stained with FasII antibody. **d** Normally developed α, β and γ lobes in control flies. **e** Severely deformed mushroom body exhibiting absence of γ lobe in *Elav-GAL4*-driven expression *SCA3trQ78(S)*. **f** Refurbishment of mushroom body phenotypes upon coexpression of InR-CFP with clearly visible γ lobes. **g** Normally developed α, β and γ lobes in control flies. **h** Degenerated mushroom body showing reduction in size and absence of parts of lobes upon 201Y-GAL4-driven expression of *SCA3trQ78(S)*. Arrow and arrowhead in e, h represent degeneration of α and γ lobe respectively. **i** Improved mushroom body morphology upon coexpression of InR-CFP in poly(Q) background. **j** Graph showing comparative analysis of the total length (± SD) of mushroom bodies dissected from adult brains of various genotypes. (Scale bars: **d**–**i** = 100 μm; ** = $P < 0.01$)

suppressor capability of InR in this tissue as well. It should be noted here that due to unavailability of a suitable third chromosome InR.Exel stock and the presence of all other transgenes on the second chromosome, the following set of experiments were carried out with the *InR-CFP* transgenic line.

In agreement with the earlier report [21], pan neuronal expression of *UAS-SCA3trQ78(S)* using *Elav-GAL4* led to almost 100% lethality at late pupal stage with only 0.5% adult eclosions being recorded (Fig. 4b; $n = 577$), whereas the control *Elav-GAL4/+* flies exhibited ~ 99.8% eclosions (Fig. 4b; $n = 525$). Ectopic expression of InR-CFP in disease background led to partial but noteworthy suppression of lethality with almost 22% of flies eclosing as adults (Fig. 4b; $n = 492$). Further, mushroom body-specific expression of *SCA3trQ78(S)* using *201Y-GAL4* resulted in only ~ 2% adult eclosions (Fig. 4b; $n = 456$) in comparison to 99% eclosions in the control *201Y-GAL4/+* population (Fig. 4b, $n = 450$). Intriguingly, coexpression of InR-CFP in *UAS-SCA3trQ78(S)/201Y-GAL4* background resulted in dramatic survivability and ~ 93.5% pupae eclosed as adults (Fig. 4b; $n = 335$). Subsequently, the longevity of the rescue flies so obtained in both the cases was assessed in comparison to the wild type flies. Compared to wild type which survived up to a maximum of 60 days post eclosion (Fig. 4c; $n = 375$), the *UAS-SCA3trQ78(S)/Elav-GAL4;UAS-InR-CFP/+* flies managed to survive to a maximum of 25 days (Fig. 4c; $n = 492$) and *UAS-SCA3trQ78(S)/201Y-GAL4;UAS-InR-CFP/+* flies survived for as much as 45 days post eclosion (Fig. 4c; $n = 335$). Importantly, both these sets of flies displayed normal behaviour during first 10–15 days and gradually developed mild paralytic phenotype.

The mushroom body is a paired organ present in the *Drosophila* brain and is composed of kenyon cells and its axonal projections namely α/α', β/β' and γ lobes [38]. Comprehensive analysis of the mushroom body was carried out by staining with Fasciclin-II which is a marker of the axons/neuropiles of neurons [39]. Compared to normally developed mushroom body in *Elav-GAL4/+* flies (Fig. 4d, j; average size = 373.36 ± 7.27 μm; $n = 46$), pan neuronal expression of *UAS-SCA3trQ78(S)* led to serious deterioration of the mushroom body in surviving adults (Fig. 4e, j, average size = 206 ± 9.2 μm; $n = 27$), which was significantly prevented upon coexpression of InR-CFP (Fig. 4f, j, average size = 343.89 ± 7.69 μm; $n = 28$). Interestingly, the neuropile of the γ lobe of the mushroom bodies of *UAS-SCA3trQ78(S)/Elav-GAL4* flies was poorly stained which might be attributed to selective loss of their neuronal counterparts in the kenyon cells (Fig. 4e). This condition was restored in mushroom bodies examined from *UAS-SCA3trQ78(S)/Elav-GAL4;UAS-InR-CFP/+* flies and the γ lobe was found to be appropriately stained in these tissues (Fig. 4f). As opposed to the apparent deformation of the mushroom body in *Elav-GAL4*-driven disease condition, expression of *SCA3trQ78(S)* using *201Y-GAL4* resulted in severe degeneration and considerable reduction in the size of the α and β neuropiles of mushroom body in surviving *UAS-SCA3trQ78(S)/201Y-GAL4* adults (Fig. 4h, j; average size = 127.84 ± 9.53 μm; $n = 38$). Moreover, overall intensity of staining was low in this case as compared to controls. Intriguingly, overexpression of InR-CFP in SCA3 expressing brain tissues resulted in almost complete suppression of degeneration with evident restoration of staining pattern as well as overall size of the α and β lobes (Fig. 4i, j; average size = 320.42 ± 8.94 μm; $n = 40$). Above findings collectively suggest that the neuroprotective capability of InR against poly(Q)-induced toxicity is equally effective in different neuronal tissues and organs.

InR Suppresses Neurotoxicity in Other Forms of Poly(Q) Disorders

The rescue potential of InR was further assessed in other forms of poly(Q) disorders using two independent HD transgenic lines—*UAS-HttQ138-mRFP* and *UAS-Htt93Q*. The former expresses an RFP tagged Htt protein containing 138 CAG repeats [26] whereas the latter harbours 93 CAG repeats in the Htt gene [27]. Phenotypically, *GMR-GAL4* driven expression of *UAS-HttQ138-mRFP* does not produce any changes in the eye as compared to the control *GMR-GAL4/UAS-HttQ15-mRFP* flies (Fig. 5a–c). However, deep pseudopupil imaging revealed that in comparison to controls (Fig. 5d), *GMR-GAL4/+;UAS-HttQ138-mRFP/+* flies confronted drastic loss of photoreceptors (Fig. 5e) with only diffused impressions of photoreceptors visible in each ommatidia (arrows in Fig. 5e). Overexpression of InR in disease background restored the status of photoreceptors with clear cut prominence of at least 4–5 photoreceptors in each ommatidia (Fig. 5f).

In case of *Htt93Q*, driving with *GMR-GAL4* produces a degenerated eye with loss of pigmentation and apparent reduction in eye size (Fig. 5h). The *UAS-Htt93Q-GMR-GAL4* flies also exhibited visible patches of roughness which progressively increased with age. When InR was coexpressed, a marked rescue in the disease phenotype was noted with restoration of the eye size, improvement in the pigmentation as well as reduction in roughness (Fig. 5i). Internal examination by toluidine blue staining in the eye sections of diseased flies suggested extensive degeneration of retinal segments with only residual mass of retinal tissue present underneath the ommatidial facet (Fig. 5k) whereas upregulation of InR reinstated the structure of the retina to a considerable extent, though the retinal projections failed to extend up to the lamina (Fig. 5l).

Taken together, these studies demonstrate that InR is capable of rescuing poly(Q)-mediated neurotoxicity in forms other than SCA3 also.

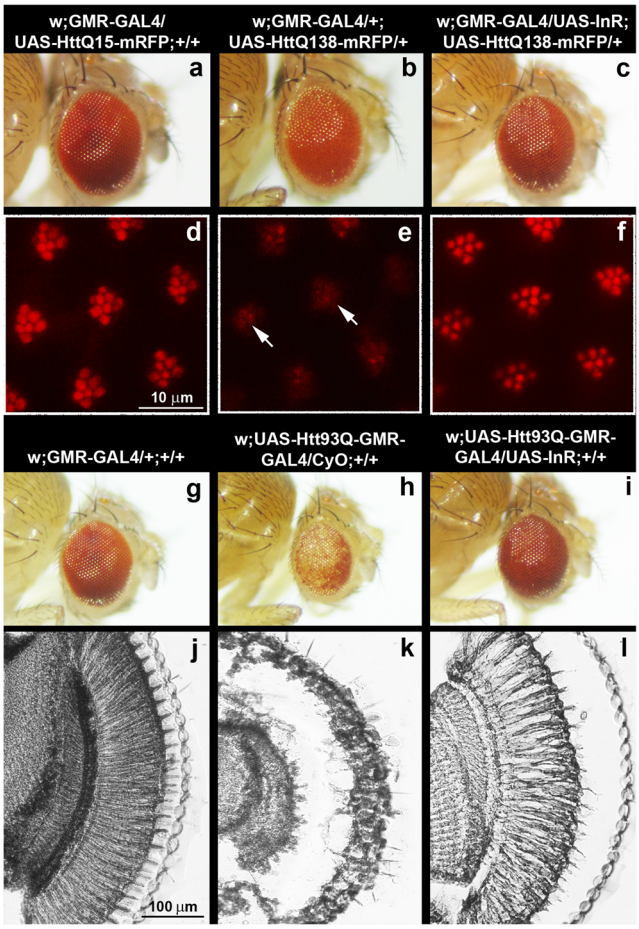

Fig. 5 Targeted overexpression of InR alleviates disease phenotypes in other forms of poly(Q) also. **a**–**c** Bright field pictures of external surface of the adult eye. *GMR-GAL4*-driven expression of *HttQ15-mRFP* or *HttQ138-mRFP* does not produce any visible phenotypes in external eye morphology nor does the coexpression of InR. **d**–**f** Deep pseudopupil images of adult eye. **d** Presence of seven photoreceptors in controls fly eyes. **e** Degeneration of photoreceptors due to expression of *HttQ138-mRFP* (arrows). **f** Restored status of photoreceptors following coexpression of InR. **g**–**i** Bright field pictures of external surface of the adult eye. **g** *w;GMR-GAL4/+;+/+* control. **h** Degenerated adult eye with loss of pigmentation and roughening of eye surface upon expression of *Htt93Q*. **i** Re-established eye structure and morphology following coexpression of InR. **j**–**l** Toluidine blue-stained horizontal sections of eye retina. **j** *w;GMR-GAL4/+;+/+* control. **k** Degenerated retinal mass due to expression of *Htt93Q*. **f** Suppression of retinal degeneration and restored internal eye architecture upon coexpression of InR. (Scale bars: **d**–**f** = 10 μm; **j**–**l** = 100 μm)

Enhanced Level of InR Suppresses Poly(Q)-Mediated Apoptosis and Cellular Stress and Induces Autophagy

Poly(Q)-induced apoptotic cell death as a result of formation of highly toxic inclusion bodies in selective regions of the brain has been long known to be the underlying cause of neuronal demise and subsequent degeneration [11, 40]. Accumulation of poly(Q) aggregates in the cell leads to activation of initiator caspases which are otherwise disabled by binding with inhibitor of apoptosis proteins like IAP1, and these initiators in turn cleave and trigger the effector caspases [11, 41, 42]. In order to examine the effect of InR upregulation in cellular apoptosis, third instar larval eye discs were subjected to acridine orange (AO) staining which labels dead cells by virtue of its property of binding to fragmented DNA [43]. While cell death was not apparent in control eye discs (Fig. S5a), *UAS-SCA3trQ78(S)-GMR-GAL4* discs showed pronounced number of dead cells throughout the eye field (Fig. S5b). Interestingly, targeted expression of InR in poly(Q) expressing cells significantly reduced the prevalence of AO positive signals indicating moderation of apoptotic events (Fig. S5c).

In order to substantiate the above observation, TUNEL assay was performed in the eye discs as well as adult eye sections. The TUNEL assay is used to label the terminal ends of fragmented DNA by terminal deoxynucleotidyl transferase (TdT) enzyme and thereby, to identify the population of apoptotic cells. Compared to the negligible TUNEL positive cells in *GMR-GAL4/+* eye discs (Fig. 6a), robust presence of TUNEL positive puncta was noted in *UAS-SCA3trQ78(S)-GMR-GAL4* eye discs which was confined to the region posterior to the morphogenetic furrow (arrows in Fig. 6b). Coexpression of InR in disease background led to substantial diminution in TUNEL positive signals (Fig. 6c). An average of 21 TUNEL positive cells could be detected per eye disc of SCA3 expressing flies as opposed to only 3 per disc when InR was upregulated (Fig. 6p). Similar results were obtained on subjecting adult eye sections to TUNEL assay (Fig. S5d–f).

Above observations were further verified by staining the third instar larval eye discs with anti-cleaved caspase-3 antibody which recognises the *Drosophila* Drice and Dcp-1 effector caspase proteins [44]. Basal level of caspase staining was evident in *GMR-GAL4/+* eye discs signifying developmentally regulated cell death (Fig. 6d, q) whereas *GMR-GAL4* driven expression of *SCA3trQ78(S)* resulted in substantial increase in the amount of caspase-3 staining in the region posterior to the morphogenetic furrow (arrow in Fig. 6e, q) pointing towards robust activation of apoptotic cascade in the target tissue (Fig. 6q). On the contrary, overexpression of InR in *UAS-SCA3trQ78(S)-GMR-GAL4* background was found to inhibit apoptotic events as a low level of caspase-3 staining confined to only a few cells in the eye region of the disc was achieved (Fig. 6f, q). Altogether, above observations comprehensively demonstrate that tissue-specific upregulation of InR dominantly reduces caspase activation and cellular apoptosis in poly(Q) disease background.

The cellular toxicity generated due to aggregation of misfolded proteins in poly(Q) disorders results in the induction of stress inducible molecular chaperone HSP70 [21, 45]. Hence, cellular abundance of HSP70 was assessed in order to investigate the stress levels in the cell and the protective effect of InR against such toxicity. In agreement with earlier reports [46], expression of cytoplasmic HSP70 was not detected in

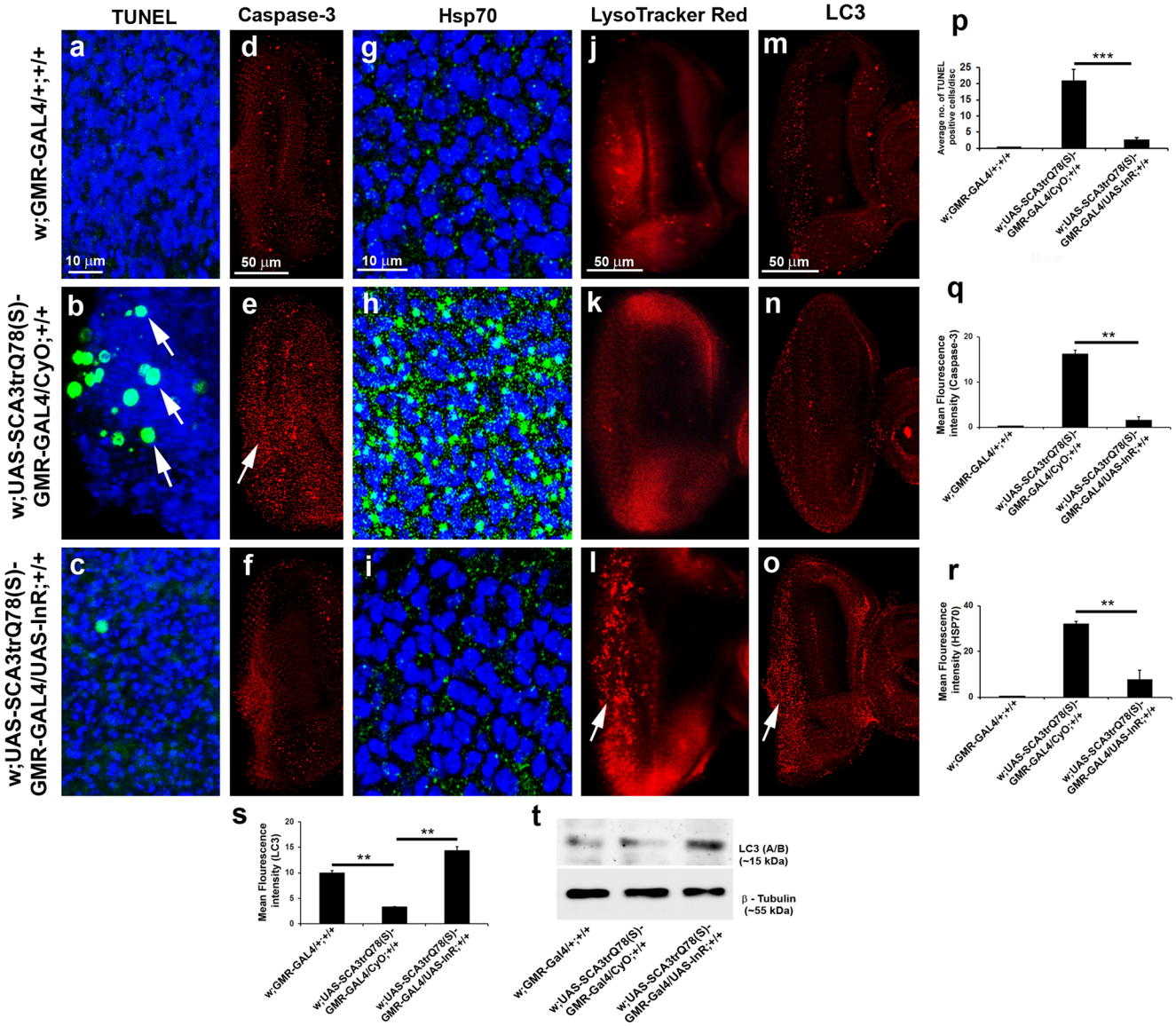

Fig. 6 Overexpression of InR suppresses poly(Q)-induced cellular stress and apoptosis and induces autophagic processes. **a**–**c** Confocal images of larval eye discs subjected to TUNEL assay. **a** Absence of TUNEL positive cells in control eye discs. **b** Appearance of TUNEL positive signals (arrows) in poly(Q) expressing eye discs. **c** Reduction in TUNEL signals in tissues coexpressing InR in disease background. **d**–**f** Confocal images of larval eye discs stained for cleaved caspase-3. **d** Absence of caspase-3 staining in control eye discs. **e** Induced expression of caspase-3 (arrow) in *UAS-SCA3trQ78(S)-GMR-GAL4/CyO* flies. **f** Reduction in caspase-3-positive cells upon coexpression of InR. **g**–**i** Confocal images of larval eye discs stained for HSP70. **g** Expression of stress-inducible HSP70 is not noted in control eye discs. **h** *GMR-GAL4*-driven expression of *UAS-SCA3trQ78(S)* induced widespread expression of HSP70. **i** Considerably reduced HSP70-positive signals upon coexpression of InR. **j**–**l** Fluorescence images of larval eye discs stained with LysoTracker Red. **j** Basal level autophagy signals observed in control eye discs. **k** Compromised autophagy in poly(Q) expressing tissues. **l** Overexpression of InR substantially induced autophagy (arrow). **m**–**o** Confocal images of larval eye discs stained for LC3. **m** Control tissues showing few LC3 positive cells. **n** Suppressed autophagy in SCA3 disease condition. **o** Marked increase in autophagic signals (arrow) following coexpression of InR. **p** Histogram representation of relative number of TUNEL positive cells per eye disc. **q** Histogram representation of relative caspase-3 fluorescence intensities. **r** Histogram representation of relative HSP70 fluorescence intensities. **s** Histogram representation of relative LC3 fluorescence intensities. **t** Western blot for protein lysates from adult heads of different genotypes probed for LC3 also confirmed enhanced level of autophagy upon upregulation of InR in poly(Q) expressing tissues. (*Scale bars*: **a**–**c**, **g**–**i** = 10 μm; **d**–**f**, **j**–**l**, **m**–**o** = 50 μm; ** = $P < 0.01$; *** = $P < 0.001$)

GMR-GAL4/+ eye discs as the flies were raised in unstressed conditions (Fig. 6g, r). However, eye-specific expression of *SCA3trQ78(S)* led to large-scale induction of HSP70 in the region posterior to the morphogenetic furrow (Fig. 6h, r). Interestingly, cellular expression of stress-induced HSP70 was contained to significant levels upon coexpression of InR in *UAS-SCA3trQ78(S)-GMR-GAL4* background with only a few HSP70-positive signals evident in the eye region of the disc (Fig. 6i, r). Thus, enhanced level of InR effectively restrains cellular stress in poly(Q) expressing cells.

Another cellular pathway that is essential for neuronal homeostasis but is affected due to poly(Q) pathology is autophagy [47–49]. Autophagy is a cellular process which disposes misfolded proteins via lysosome-mediated proteostasis [50]. With respect to neurodegenerative disorders, autophagy has been implicated as the major degradation pathway for aggregation-prone proteins [51]. Knockdown of autophagy genes has been shown to promote aggregation of misfolded protein [52, 53] whereas their upregulation protects against neurodegeneration in HD mouse models [54, 55]. Moreover, it has also been demonstrated that insulin signalling may be implicated in the promotion of autophagic clearance of poly(Q) aggregates [56]. Following these lines, we investigated the effect of enhanced insulin signalling on autophagy induction in poly(Q) disease conditions. Autophagy can be monitored in *Drosophila* using the LysoTracker dye which is an acidotropic dye that stains the lysosomes as well the autolysososmes [57]. On subjecting third instar larval eye discs to LysoTracker Red, it was observed that in comparison to controls (Fig. 6j), targeted expression of *SCA3trQ78(S)* suppresses the rate of autophagy in the region posterior to the morphogenetic furrow which can be perceived in the form of red punctate signals (Fig. 6k). Upregulation of insulin signalling via overexpression of InR resulted in a marked increase in the number of autophagy signals which were explicitly localised at the posterior end of the eye disc (arrow in Fig. 6l).

The relative level of autophagy was further examined by staining and western blot analysis with LC3 antibody. The microtubule-associated protein LC3 is a mammalian homologue of Atg8 which is commonly utilised as an alternative marker to monitor autophagy [58, 59]. The two major variants of the LC3 gene family, LC3A and LC3B, constitute the main components of the autophagosomal membrane in their LC3-II form respectively [60]. On staining third instar larval eye discs with LC3A/B antibody, it was noted that *UAS-SCA3trQ78(S)-GMR-GAL4* eye discs showed reduced expression of LC3 (Fig. 6n, s) as compared to the basal level autophagic signals in *GMR-GAL4/+* control discs (Fig. 6m, s). Interestingly, coexpression of InR in poly(Q) expressing tissues increased the number of LC3-containing foci to a considerable extent (Fig. 6o, s). Moreover, their density was found to be even higher in comparison to the control eye discs (compare Fig. 6m with o). Furthermore, western blot analysis also revealed similar autophagic pattern (Fig. 6t). These findings indicate towards the plausible role of insulin signalling in inducing autophagy in poly(Q) expressing cells as a defence response against abnormally folded proteins. Collectively, it can be comprehended that upregulation of insulin signalling in poly(Q) expressing cells not only inhibits cellular stress and cell death but also induces protective mechanisms like autophagy in an attempt to eliminate anomalous proteins from the cells.

Targeted Overexpression of InR Inhibits the Formation of Poly(Q) Protein Aggregates

Formation of nuclear inclusions bodies (IBs) in affected neurons is the major pathological hallmark of poly(Q) disorders, and the size and number of these aggregates can be directly correlated with the severity of the disease [20, 21, 32]. Since inclusion bodies represent a direct measure of pathogenesis in poly(Q) diseases [61, 62], it was important to determine the potential of InR in moderating the presence of inclusions in the target tissue. For this, third instar larval eye discs were stained with anti-HA antibody as the *SCA3trQ78(S)* transgenic protein is N-terminally HA tagged. On driving *SCA3trQ78(S)* alone using *GMR-GAL4*, a robust accumulation of poly(Q) aggregates was witnessed in the region posterior to the morphogenetic furrow (Fig. 7a, c), whereas coexpression of InR along with the disease transgene led to a significant reduction in the abundance of inclusion bodies (Fig. 7b, c). Magnified images further revealed their subcellular localisation pattern and variation in size. While the aggregates in *UAS-SCA3trQ78(S)-GMR-GAL4* cells were mostly nuclear in nature and appeared as large blobs of poly(Q) proteins (arrow in Fig. 7a'), overexpression of InR caused these aggregates to be much smaller in size and majorly localised to the cytoplasmic compartment (arrows in Fig. 7b').

Above observations were corroborated by carrying out western blot analysis using protein lysates prepared from 2-day old adult flies. As reported earlier [32], protein lysates from poly(Q) expressing flies led to the formation of high molecular weight SDS-insoluble protein complexes that were difficult to resolve and therefore, predominantly remained trapped inside the stacking gel (Fig. 7d, lane 1). A noteworthy band was observed at 90 kDa which represents the oligomeric forms of poly(Q) aggregates. Following expression of InR, the abundance of the protein complexes trapped in the stacking gel was considerably reduced (Fig. 7d, lane 2). Interestingly, the 90-kDa band showed a concomitant intensification of the signal as the decrease in the stacking gel signal intensity which suggests increased solubility of the poly(Q) protein complex. Some additional bands were also observed in the resolving gel which represent other oligomeric forms of poly(Q) aggregates.

In order to substantiate whether upregulation of InR can prevent aggregate formation in other forms of poly(Q) diseases as well, the *UAS-HttQ138-mRFP* HD line was utilised. The *UAS-HttQ138-mRFP HD* transgenic line allows for in vivo imaging of Htt expression as well as its aggregation in live cells [26]. Widespread expression of Htt in the form of RFP containing aggregates was observed in the eye field of the imaginal discs of *GMR-GAL4/+;UAS-HttQ138-mRFP/+* larvae (Fig. 7e). Subsequent examination at higher magnification revealed distinct localisation of the RFP signals in the nuclear compartment (arrows in Fig. 7g), as observed in case

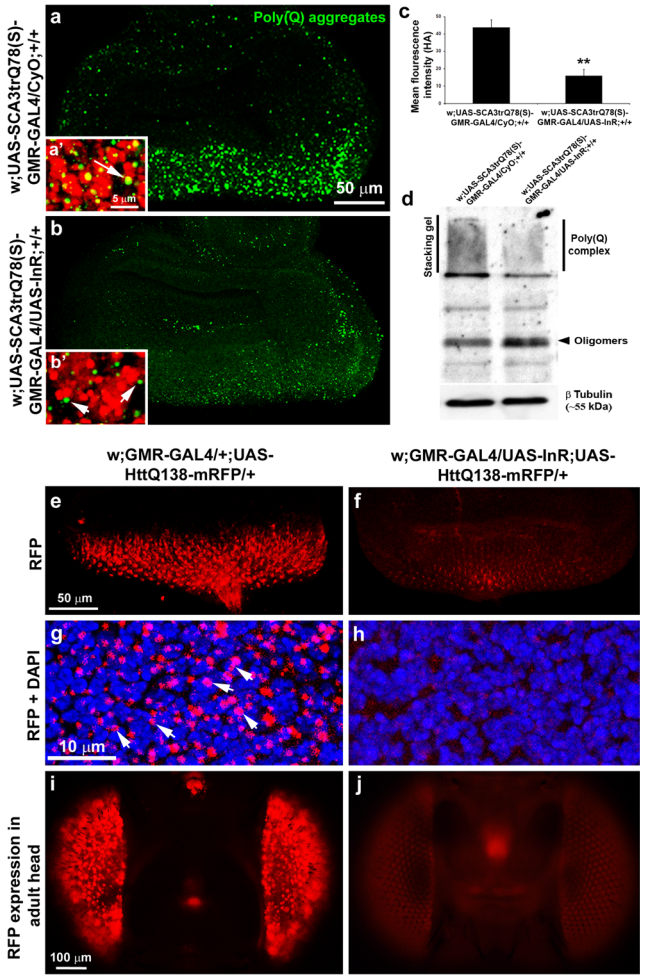

Fig. 7 Coexpression of InR suppresses poly(Q)-induced inclusion body formation in early and late stages of development. **a**–**b**, **a′**–**b′** Confocal images of larval eye discs stained with anti-HA antibody. **a**, **a′** *GMR-GAL4*-driven *SCA3trQ78(S)* transgene induced formation of inclusion bodies in the region posterior to the morphogenetic furrow that majorly localised to the nucleus. Arrow in **a′** shows nuclear location of IBs. **b**, **b′** Significant reduction in inclusion body formation upon coexpression of InR with residual aggregates restricted to the cytoplasm. Arrows in **b′** show cytoplasmic location of IBs. **c** Histogram representation of relative fluorescence intensities of HA staining. **d** Western blot for protein lysates from adult heads of disease v/s rescue genotypes probed with HA antibody. **e**–**h** Confocal images of larval eye discs examined for mRFP expression. **e** Eye field-specific aggregate formation caused by *GMR-GAL4*-driven expression of *UAS-HttQ138-mRFP*. **f** Reduced aggregate formation and therefore lowered mRFP expression upon coexpression of InR, **g** mRFP containing poly(Q) aggregates predominantly localised to the nucleus (arrows), **h** Significant prevention of inclusion body formation upon coexpression of InR with remaining aggregates confined to the cytoplasm. **i**–**j** Fluorescence images of adult heads assessed for mRFP expression. **i** Robust expression of *HttQ138Q-mRFP* is indicative of aggregate formation throughout the adult eye. **j** Absence of mRFP expression upon coexpression of InR suggests inhibition of aggregate formation. (*Scale bars*: **a**–**b**, **e**–**f** = 50 μm; **a′**–**b′** = 5 μm; **g**–**h** = 10 μm; **i**–**j** = 100 μm; ** = $P < 0.01$)

of SCA3 (Fig. 7a′). On the contrary, *GMR-GAL4/UAS-InR;UAS-HttQ138-mRFP/+* eye discs displayed a momentous decrease in the number of *Htt-RFP* aggregates and whatever few were present were primarily localised to the posterior tip of the eye disc only (Fig. 7f). In this context, it is also important to note that the residual RFP signal was found to be largely cytoplasmic in nature (Fig. 7h), thereby, reaffirming the previous observations. Subsequently, the investigations were further extended to adult stages, wherein adult heads of the respective genotypes were decapitated and directly visualised under fluorescence microscope for in-vivo observation of the aggregates. Inevitably, compared to the *GMR-GAL4/+* flies, 2-day-old adult heads of *GMR-GAL4/+;UAS-HttQ138-mRFP/+* flies showed bright red fluorescing puncta throughout the eye portion of the head (Fig. 7i). Distinct large globular signals were evident in most of the ommatidia indicative of the existence of inclusion bodies all over the eye field. Conversely, on overexpressing InR in poly(Q) expressing cells, there was a clear absence of the red punctate signals in the eye with minor inclusions noted in very few eyes (Fig. 7j).

Above results clearly suggest that enhanced level of InR suppresses the poly(Q)-induced neurotoxicity by modulating the abundance, distribution dynamics and solubility of the inclusion bodies.

InR-Mediated Mitigation of Poly(Q) Toxicity Is Not a Consequence of Induced Cell Proliferation

Insulin signalling via the insulin receptor has been long known to be involved in cellular growth and proliferation [63]. Moreover, it has been implicated as one of the major pathways in cancer cell proliferation [64, 65]. In *Drosophila*, the insulin signalling pathway stands out as an important regulator of cellular proliferation and size, especially during imaginal disc development [66, 67]. In view of above, it was essential to determine whether the enhanced level of InR confers rescue by replenishment of the degenerating neuronal cells via cell cycle re-entry or not. For this, BrdU incorporation assay was carried out in third instar larval eye discs of SCA3 expressing flies, which is a test for DNA replication during S phase of the cell cycle [68]. In eye discs dissected from *GMR-GAL4/+* control larvae, the second mitotic wave region displayed robust BrdU incorporation as it contains cells undergoing mitosis and is present just below the morphogenetic furrow [69, 70] (arrow in Fig. 8a). In case of *UAS-SCA3trQ78(S)/GMR-GAL4* eye discs, compromised BrdU incorporation was observed with evident lack of staining at some places (arrow in Fig. 8b). This may be attributed to the impaired transcriptional efficiency and the intrinsic toxicity in these cells [37]. In contrast, coexpression of InR in disease background led to improvement in BrdU incorporation to levels as good as the control discs (arrow in Fig. 8c). Notably, BrdU incorporation in other parts of the eye disc remained unaffected in all the three genotypes. These results indicate that the rescue mechanism does not entail cell

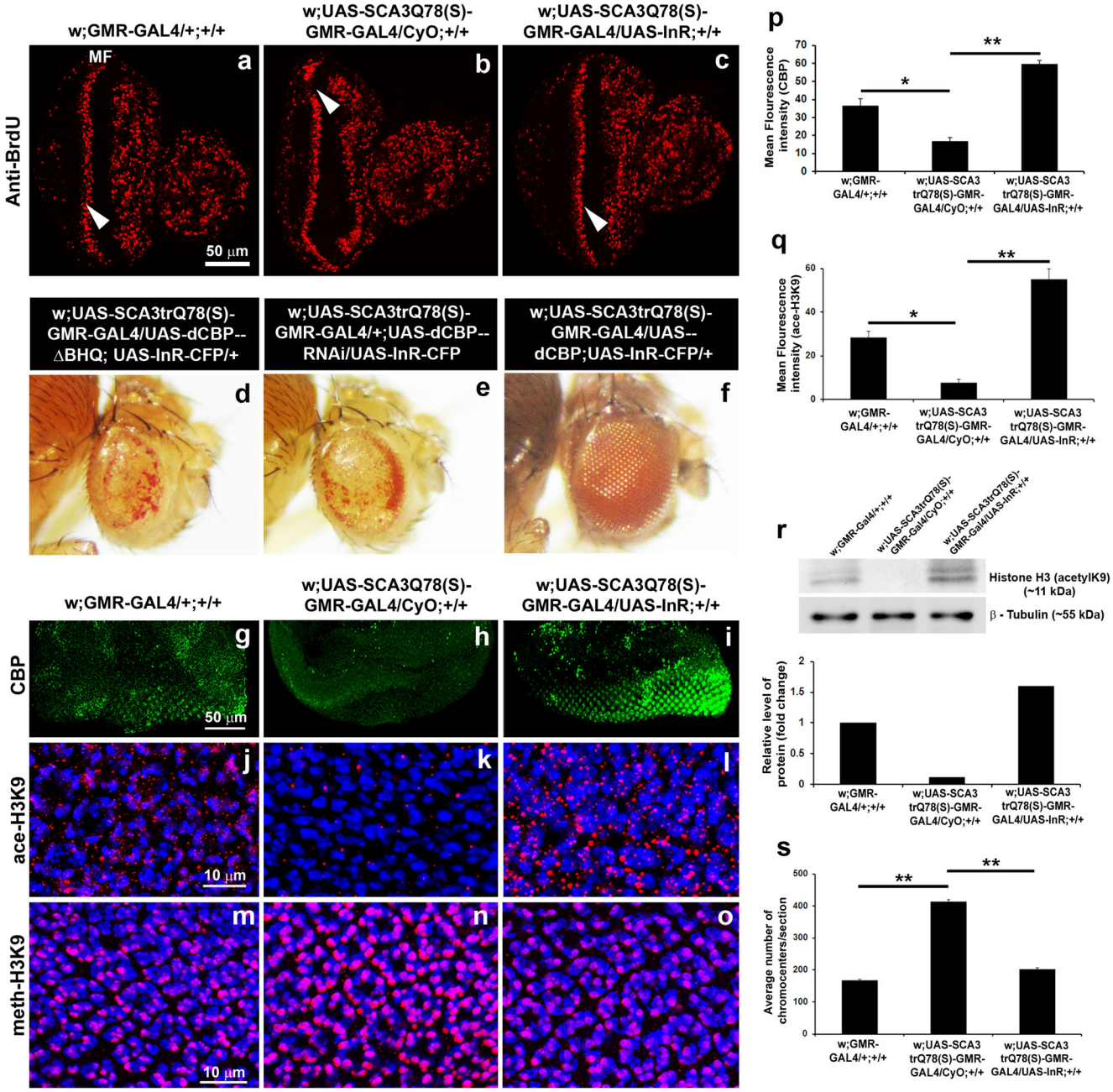

Fig. 8 Enhanced expression of InR does not induce cellular proliferation but modulates the expression of CBP via chromatin remodelling to drive rescue of poly(Q)-induced neurotoxicity. **a**–**c** Confocal images of larval eye discs stained with anti-BrdU. **a** *w;GMR-GAL4/+;+/+* shows most of the BrdU incorporation in the second mitotic wave region (arrowhead), just below the morphogenetic furrow. **b** Inconsistent incorporation of BrdU following expression of *SCA3trQ78(S)* transgene (arrowhead). **c** Coexpression of InR does not induce additional cell proliferation but restores poly(Q)-mediated defects in BrdU incorporation. **d**–**f** Bright field pictures of external surface of the adult eye. **d**, **e** InR-induced rescue of poly(Q) neurodegeneration is averted by downregulating dCBP using *dCBPΔBHQ* and *dCBP-RNAi*. **f** Additive rescue of poly(Q)-induced toxicity upon coexpression of InR-CFP and dCBP in SCA3 background. **g**–**i** Confocal images of larval eye discs stained for dCBP. **g** Basal level expression of dCBP in control eye discs. **h** Reduced expression of dCBP in poly(Q) disease conditions. **i** Enhanced dCBP expression in the region posterior to the morphogenetic furrow (arrow) following coexpression of InR in SCA3 background. **j**–**l** Confocal images of larval eye discs stained for Histone H3 (acetylK9). **j** Basal level histone acetylation in control eye discs. **k** Reduced expression of ace-H3K9 following expression of *SCA3trQ78(S)* transgene. **l** InR overexpression restored ace-H3K9 expression with the levels being greater than the controls. **m**–**o** Confocal images of larval eye discs stained for Histone H4 (methylK9). **m** Basal level meth-H4K9 staining in control. **n** Enriched heterochromatin in *SCA3* expressing eye discs. **o** Loss of heterochromatin following coexpression of InR in disease background. **p** Histogram representation of relative CBP fluorescence intensities. **q** Histogram representation of relative ace-H3K9 fluorescence intensities. **r** Western blot for protein lysates from adult heads of different genotypes probed for ace-H3K9, histogram representation of relative ace-H3K9 protein levels (fold change). **s** Histogram representation of relative number of chromocenters per section. (*Scale bars*: **a**–**c**, **g**–***i*** = 50 μm; **j**–**o** = 10 μm; * = $P < 0.05$; ** = $P < 0.01$)

division and formation of new cells to account for the dead ones but some other aspect of InR function is mediating the suppression of poly(Q)-induced neurotoxicity and cellular damage.

Upregulation of InR Restores the Expression of CBP and Level of Histone Acetylation and Moderates the Abundance of Heterochromatin

One of the important transcription factors sequestered inside the inclusion bodies is the CREB binding protein or CBP [71]. The resulting interference in CBP mediated transcription leads to cellular toxicity and retinal degeneration in *Drosophila* models of poly(Q) diseases [10, 72]. In view of the fact that the insulin signalling pathway is one of the major upstream regulators of CBP functioning, we wanted to examine the effect of modified expression of CBP in disease condition in conjunction with overexpressed InR. Genetic interaction studies were carried out using two independent dCBP mutant lines—*UAS-dCBP-ΔBHQ* and *UAS-dCBP-RNAi*. The *CBP-ΔBHQ* transgenic line exhibits a deletion in the acetyltransferase as well as the zinc finger domain and *CBP-RNAi* uses RNA interference in order to knock down the levels of CBP [28, 73]. Eye-specific downregulation of CBP by using *UAS-dCBP-ΔBHQ* or *UAS-dCBP-RNAi* led to degeneration of the adult eye in both the cases in comparison to *GMR-GAL4/+* controls (Fig. S6, compare b, c with a). Subsequently, reduced expression of CBP either by *dCBP-ΔBHQ* or *UAS-dCBP-RNAi* in *SCA3trQ78(S)* expressing flies further aggravates the neurodegenerative phenotype (Fig. S6, compare e, f with d). Extrapolation of these studies to increased InR expression in *UAS-SCA3trQ78(S)-GMR-GAL4/UAS-dCBPΔBHQ* or *RNAi* background revealed containment of the rescue potential of InR in both the cases (Fig. 8d, e). Above observations suggest that the downstream upregulation of CBP due to enhanced level of InR was prevented by CBP-RNAi or rendered inoperative by CBP-ΔBHQ. Intriguingly, it appears that concurrent upregulation of CBP as well as InR leads to a rescue event much better than that achieved with InR alone and the eyes appeared as good as the control (Fig. 8f). This implies additive protection against poly(Q)-induced neurotoxicity and suggests that a threshold level of CBP is required in the cell for achieving the InR-mediated suppression of poly(Q)-induced neurotoxicity.

In order to substantiate if InR-mediated rescue event is indeed mediated by CBP, third instar larval eye discs were stained with anti-dCBP antibody [30]. A basal level of CBP expression was observed throughout the eye disc of the control *GMR-GAL4/+* larvae (Fig. 8g, p). Interestingly, a marked decrease was evident in the eye field upon driving the expression of *SCA3trQ78(S)* (Fig. 8h, p) which suggests compromised transcriptional machinery in the poly(Q) expressing cells. Quite evidently, in *UAS-SCA3trQ78(S)-GMR-GAL4/UAS-InR* eye discs, the abundance of CBP was found to be elevated in the eye field and the signal intensity was even greater than the control *GMR-GAL4/+* discs (Fig. 8i, p).

InR induces growth-promoting signals in the cell on binding of its ligand, the *Drosophila* insulin-like peptides or dilps [74]. "Growth" is a by-product of increased cellular transcription which occurs as a result of various histone modification events. A link has been established between the insulin signalling pathway and several specific histone modifications such as Histone H3 acetylation [75] as well as methylation [76] indirectly through the phosphoinositide-3-Kinase (PI3K) enzyme. As discussed above, since the InR mediated rescue mechanism does not involve enhanced cellular proliferation, therefore, it was important to assess if enhanced level of InR confers rescue by restoring the compromised transcriptional machinery in poly(Q)-expressing cells. For this, the level of histone acetylation as well as methylation was examined in third instar larval eye discs. The former was evaluated by staining with anti-Histone H3 acetylK9 (ace-H3K9) antibody. It was discerned that in comparison to a basal level of staining in *GMR-GAL4/+* tissues, *UAS-SCA3trQ78(S)-GMR-GAL4* eye discs revealed a noteworthy decrease in the abundance of acetylated histone H3 in the nucleus (compare Fig. 8j with k, also see 8q). Interestingly, coexpression of InR augmented the level of acetylated histone to a significant extent both in terms of staining intensity as well as abundance of signal (Fig. 8l, q). Western blot analysis also yielded similar results (Fig. 8r). Subsequently, on staining with anti-Histone H3 methylK9 (meth-H3K9) for assessing the status of histone methylation, contrasting pattern was observed. Whereas control tissues showed a basal level of histone methylation (Fig. 8m), poly(Q) expression using *GMR-GAL4* driver, caused a substantial upsurge in the staining levels, confined to the nuclear compartment only (compare Fig. 8m with n). This suggests an increase in the heterochromatization and reduced cellular transcription due to poly(Q)-mediated toxicity. Interestingly, when InR was upregulated in poly(Q) background, the staining was restored to control levels indicating loosening up of the heterochromatin (Fig. 8o). Also, on counting the average number of nuclei with the chromocenter per section of the eye disc in each case, it was noted that upregulation of InR resulted in a significant reduction in the number of positive chromocenters by approximately 50% in comparison to poly(Q) expressing tissues (Fig. 8s). Cumulatively, above findings suggest that InR-mediated rescue of poly(Q)-induced neurodegeneration is being achieved by restoration of the cellular abundance of CBP and improved rate of global transcription via increased histone acetylation and decreased methylation.

Discussion

We have demonstrated earlier that tissue-specific upregulation of *Drosophila* Myc (dMyc) dominantly suppresses poly(Q)-mediated neurotoxicity and could be utilised as a drug target. While screening for additional genetic modifiers of poly(Q) to be used as a drug target in a combinatorial manner with dMyc, the insulin signalling pathway appeared as a promising candidate to review in this context owing to its well-known role in regulation of growth and metabolism of neuronal tissues and the fact that *myc* is an established downstream effector of this pathway [13, 15, 18]. Since poly(Q) disorders manifest due to widespread neuronal death in the brain and nervous system, it was hypothesised that growth-promoting signals via upregulation of the insulin signalling pathway may provide survival signals to the dying cells and help alleviate neurodegeneration. Consistent with the hypothesis, we report for the first time that targeted overexpression of *Drosophila* insulin receptor, InR (*Drosophila* homologue of the human insulin-like growth factor 1 receptor, IGF1R), could significantly suppress poly(Q)-induced disease phenotypes and neurotoxicity in *Drosophila*. Moreover, the protective capacity of InR was found to persist through age which is important in light of the fact that the severity of neurodegenerative disorders tends to worsen with age [77]. Downregulation of InR, on the other hand, caused exaggeration of the disease phenotype. It is of note that InR not only rescued cellular degeneration but also exhibited the capability of preventing the accumulation of poly(Q) inclusion bodies. The rescue potential of InR was found to be equally effective in both the eye and the neurons of the central and the peripheral nervous system and the neurotoxicity suppression by InR also well-translated into functional rescue.

The *Drosophila* insulin-like peptides (dilps) exert their effects by binding to the insulin receptor (InR), a member of the family of receptors known as receptor tyrosine kinases that contain ligand-activated tyrosine kinase activity within their cytoplasmic domains. The first half of the InR protein constitutes the α subunit that harbours the ligand binding site while the latter half is referred to as the β subunit and contains the transmembrane region and autophosphorylation sites [78]. The InR ORF is highlighted by the conservation of the potential insulin-binding and tyrosine kinase domains, as well as a transmembrane domain preceding the tyrosine kinase domain [78]. Notably, the region encoding the tyrosine kinase domain, containing the primary sites of autophosphorylation and autoactivation, is conserved between InR and IGF1R [79]. Therefore, the *Drosophila* InR undergoes autophosphorylation and activation in a manner similar to the human insulin receptor. The InR protein is abundantly expressed during embryogenesis and its function is required for normal development. Moreover, loss of function in InR induces pleiotropic phenotypes in the development of the embryonic nervous system [78].

Interestingly, impaired IGF-R signalling has been implicated in a variety of neurodegenerative disorders [35]. Moreover, reduced levels of IGF-R mRNA as well as protein in these disorders also suggests a plausible role of IGF-R signalling in their pathogenesis [16, 17]. In *Drosophila*, binding of dilps to InR results in the activation and downstream functioning of the insulin signalling pathway [18]. In agreement to the earlier reports, we also found a significant reduction in the expression of InR in poly(Q) expressing tissues. Targeted upregulation of InR in the developing *Drosophila* eye has been demonstrated to cause cell autonomous overgrowth of the eye [80]. Consistently, *GMR-GAL4*-driven overexpression of InR resulted in eye size enlargement and that in poly(Q) background led to suppression of neurodegeneration. Since BrdU incorporation efficiency revealed absence of any kind of neuronal differentiation, it was perceived that mitigation of the poly(Q)-induced toxicity was being achieved by the intrinsic growth promoting properties of InR.

Having a basic idea like this, and in lieu of further elaborating upon the mechanistic details of the rescue mechanism, the status of cellular stress and apoptosis were analysed as these are the key events responsible for neuronal loss in poly(Q) disorders. Misfolded poly(Q) proteins induce cellular stress which leads to expression of HSPs, majorly HSP70, which in turn activate cysteine caspases and trigger apoptosis and neuronal demise [42, 81]. Overexpression of InR resulted in significant reduction in cellular stress and effectively suppressed apoptotic events in early as well as late stages of disease progression as indicated by reduced HSP70 and TUNEL, caspase staining in rescue flies.

Interestingly, there appeared a possibility of autophagy-mediated protection against poly(Q)-induced pathology as the rescue samples exhibited enhanced expression of LC3 and LysoTracker staining. Since autophagy is frequently induced as a result of growth factor deprivation whereas in this case the cells are being enriched with growth promoting signals, we suspect that the observed upsurge in autophagy signals might be primarily due to chaperone-mediated autophagy (CMA) or aggrephagy. CMA is a type of autophagy that functions to eliminate erroneous or unused proteins from the cell by means of a CMA-substrate/chaperone complex. The chaperones help unfold the substrate protein and translocate it across the lysosomal membrane where it is degraded with the help of lysosomal hydrolases [82]. Aggrephagy, on the other hand, is a process of selective autophagy that comes into play when there is a failure in the processing of misfolded proteins via the chaperones or the proteasomal degradation system. Aggrephagy degrades ubiquitin-labelled aggregated proteins by docking-specific cargos to the autophagosome with the help of ubiquitin-binding cargo receptors that bind to Atg8/Atg8 homologues (like LC3) which in turn causes the

closure of the autophagosome and degradation of the contents thereafter [83, 84]. This process is selective for sequestration of protein aggregates and is mediated after intended chaperone-assisted protein aggregate formation and their recognition by ubiquitin E3 ligases that aids the formation of autophagosomes. Based on the preliminary data presented above, it is difficult to judge which arm of the autophagic pathway might be functioning to decrease the aggregate load in the cell and therefore, further studies need to be focussed on deciphering the exclusive chaperones as well as E3 ligases that function to mark the poly(Q) proteins for autophagy and aid their downstream degradation.

Since the poly(Q) aggregates appear to be selectively targeted for degradation, it was imperative to assess the status of poly(Q)-containing inclusion bodies in disease v/s rescue samples. Overexpression of InR caused a significant reduction in the SDS-insoluble poly(Q) aggregates and a similar intensification of soluble forms of poly(Q) proteins which we believe to be the oligomeric poly(Q) species. Immunostaning experiments revealed that the residual inclusion bodies in the rescue samples mostly remained restricted to the cytoplasmic compartment of the cell as opposed to widespread nuclear inclusions observed in case of disease. Given the fact that cytoplasmic inclusion bodies are considered to be less toxic than their nuclear counterparts [21] and since there appears to be a rise in the oligomeric state of poly(Q) proteins we propose that increased insulin signalling perhaps inhibits the aggregate formation and their nuclear translocation and promotes their break down into soluble forms by means which would be an interesting area of future investigations. The marked decrease in aggregate formation can be directly correlated with near complete restoration of disease associated functional deficits in addition to reinstatement of morphological and histological phenotypes. Improved survival rates, enhanced life expectancy and ameliorated vision of the adult rescue flies suggest that InR-mediated mitigation of poly(Q)-induced neurotoxicity is a multifaceted phenomenon with InR being a proficient genetic modifier.

Sequestration of essential transcriptional regulators into the inclusion bodies has been contemplated as one of the major causative factors for poly(Q)-induced cellular toxicity and neuronal dysfunction [85]. More specifically, depleted pools of the c-AMP response element binding protein (CBP) have been implicated in cellular repression of transcriptional activity eventually leading to neurotoxicity [71, 72]. Consistent with these earlier findings, we report a significant reduction in the cellular abundance of CBP following expression of SCA3 protein in the *Drosophila* system. Further, regulated overexpression of CBP or enhancement of its activity has been demonstrated to suppress poly(Q)-induced neurodegeneration [10]. In the present study also, following overexpression of InR, an increase in the expression of CBP was noted, however, it is difficult to comment at this point whether the observed activation of CBP is due to its inhibition from sequestration into the inclusion bodies or due to enhanced transcription of its gene. Genetic interaction studies further demonstrated that reduced expression of CBP in poly(Q) background restricts InR's ability to mitigate the toxicity whereas simultaneous increase in the expression of both, CBP and InR results in additive rescue of poly(Q) toxicity indicating a downstream association of CBP in InR mediated suppression of neurodegeneration.

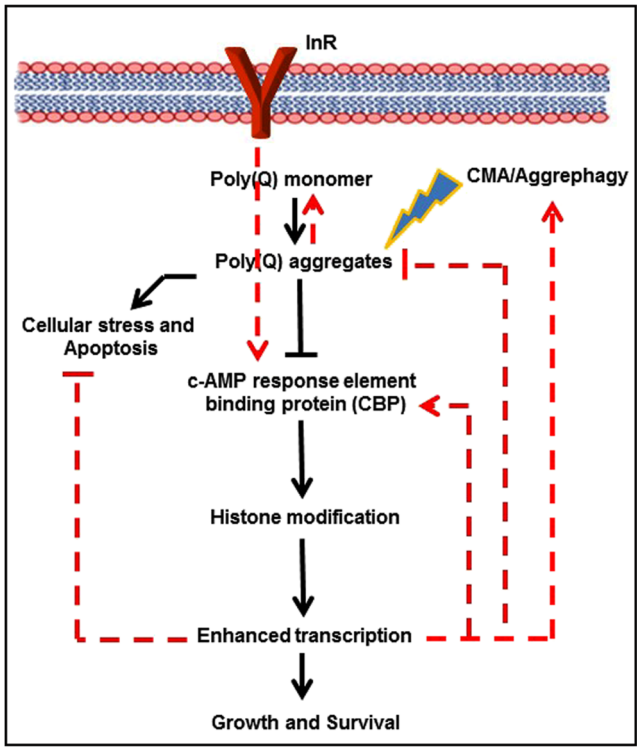

Fig. 9 Polyglutamine disorders result from formation of poly(Q) aggregates that cause neuronal dysfunction and cellular death. Poly(Q) monomers accumulate together to form poly(Q) aggregates that sequester important transcription factors like CBP and lead to cellular stress and apoptosis. We propose that InR suppresses poly(Q)-induced neurotoxicity by modulating the levels of CBP. We hypothesise that the enhanced level of CBP functions to induce histone modifications that results in enhanced transcriptional rate and eventually, improved growth and survival. The toxic effects of poly(Q) aggregates might be alleviated by reduced cellular stress and apoptosis, inhibition of formation of poly(Q) aggregates or their degradation via CMA or aggrephagy as a result of augmented rate of global transcription

In light of the fact that CBP is a potent histone acetyltransferase that works in conjunction with various other transcription factors to regulate expression of target genes via acetylation of core histone particles [86], we investigated whether InR curtails neurodegeneration employing a CBP-induced chromatin remodelling mechanism or not. Although a link has been established between the insulin signalling pathway and several specific histone modifications such as Histone H3 acetylation [75] as well as methylation [76] indirectly through the Phosphoinositide-3-

Kinase (PI3K) enzyme, no direct evidence has been put forward till date that reveals a direct implication of altered levels of the insulin receptor on chromatin remodelling. We report for the first time that overexpression of InR leads to drastic transcriptional upregulation as assessed by enhanced level of acetylation and reduced level of methylation of core histones. We therefore propose that InR facilitates global chromatin remodelling and restores the compromised transcriptional status of the cell arising due to poly(Q), thereby, enhancing the expression of various chaperones as well as transcription factors that eventually exert a concerted protective effect against the disease condition. Importantly, our study also established that overexpression of InR did not only rescue disease-associated phenotypes in case of SCA3 but also succeeded in manifesting protective effects against mutated huntingtin-induced toxicity pointing towards its potential to act as a positive modifier for other poly(Q) diseases as well. Moreover, our finding also suggests towards a possibility of testing some anti-diabetic drugs to supresses the progression of poly(Q)-mediated neurodegeneration.

In summary, we report that the *Drosophila* insulin receptor (InR) can act as a novel genetic modifier of poly(Q) diseases by improving cellular transcription and activation of genes that may either inhibit poly(Q) aggregate formation or accelerate their degradation via cellular proteostasis pathways like CMA or aggrephagy (Fig. 9). Poly(Q) aggregates exert inhibitory effects on CBP-like transcription factors, cellular ubiquitin-proteasome system and induce cellular stress and apoptosis. InR acts to stimulate histone modifications that result in an enhanced transcriptional rate leading to the release of such poly(Q)-induced inhibitory effects and promotion of growth and survival. We believe that InR-mediated improved histone acetylation was essentially being achieved by enrichment of the cellular pool of CBP which is further augmented by the upsurged transcriptional events thereby, closing the loop (Fig. 9).

Further work in the near future can focus on elaborating on how the insulin pathway can be exploited for drug development and therapeutic intervention against neurodegenerative disorders. For this, it will be interesting to reveal other candidate molecules that InR might modulate in order to bring about the chromatin remodelling. The mechanistic details would be helpful in elucidating whether InR activates the canonical insulin signalling pathway for bringing about the rescue event or some other route is undertaken for the same. It will also be fascinating to decipher the precise domain of the InR receptor that is essential but sufficient in bringing about the rescue against poly(Q)-induced neurotoxicity. Finally, it also needs to be tested whether InR exhibits similar modifier capacity against poly(Q) disorders in other model systems as well.

Acknowledgments We are thankful to J. Troy Littleton (Massachusetts Institute of Technology, USA), Hugo Stocker (Institute for Molecular Systems Biology, Switzerland), Ernst Hafen (Institute for Molecular Systems Biology, Switzerland), Justin P. Kumar (Indiana University, Bloomington, USA) and T. Lilja (Stockholm University, USA) for providing different fly stocks and some antibodies used in this study. We also thank Bloomington Stock Center, USA, for providing some fly stocks. We also thank DST-FIST(L2) support to the department. We are grateful to Ms. Nabanita Sarkar for technical support.

Funding Information This work was supported by research grants (No. BT/PR15492/MED/122/46/2016) from the Department of Biotechnology (DBT), Government of India, New Delhi, India, to S.S. KR is supported by the Senior Research Fellowship (Ref. No. Schs/SRF/AA/139/F-227/2013-14) from the University Grant Commission (UGC), New Delhi, India.

References

1. Landles C, Bates GP (2004) Huntingtin and the molecular pathogenesis of Huntington's disease. Fourth in molecular medicine review series. EMBO Rep 5(10):958–963. https://doi.org/10.1038/sj.embor.7400250
2. Everett CM, Wood NW (2004) Trinucleotide repeats and neurodegenerative disease. Brain 127(Pt 11):2385–2405. https://doi.org/10.1093/brain/awh278
3. Pearson CE, Nichol Edamura K, Cleary JD (2005) Repeat instability: mechanisms of dynamic mutations. Nat Rev Genet 6(10):729–742. https://doi.org/10.1038/nrg1689
4. Thompson LM (2008) Neurodegeneration: a question of balance. Nature 452(7188):707–708. https://doi.org/10.1038/452707a
5. Ordway JM, Tallaksen-Greene S, Gutekunst CA, Bernstein EM, Cearley JA, Wiener HW, Dure LS, Lindsey R et al (1997) Ectopically expressed CAG repeats cause intranuclear inclusions and a progressive late onset neurological phenotype in the mouse. Cell 91(6):753–763
6. Wellington CL, Ellerby LM, Hackam AS, Margolis RL, Trifiro MA, Singaraja R, McCutcheon K, Salvesen GS et al (1998) Caspase cleavage of gene products associated with triplet expansion disorders generates truncated fragments containing the polyglutamine tract. J Biol Chem 273(15):9158–9167
7. Fan HC, Ho LI, Chi CS, Chen SJ, Peng GS, Chan TM, Lin SZ, Harn HJ (2014) Polyglutamine (PolyQ) diseases: genetics to treatments. Cell Transplant 23(4–5):441–458. https://doi.org/10.3727/096368914X678454
8. Chen S, Berthelier V, Yang W, Wetzel R (2001) Polyglutamine aggregation behavior in vitro supports a recruitment mechanism of cytotoxicity. J Mol Biol 311(1):173–182. https://doi.org/10.1006/jmbi.2001.4850
9. Michalik A, Van Broeckhoven C (2003) Pathogenesis of polyglutamine disorders: aggregation revisited. Hum Mol Genet 12(2):R173–R186. https://doi.org/10.1093/hmg/ddg295
10. Taylor JP, Taye AA, Campbell C, Kazemi-Esfarjani P, Fischbeck KH, Min KT (2003) Aberrant histone acetylation, altered transcription, and retinal degeneration in a Drosophila model of polyglutamine disease are rescued by CREB-binding protein. Genes Dev 17(12):1463–1468. https://doi.org/10.1101/gad.1087503
11. Saudou F, Finkbeiner S, Devys D, Greenberg ME (1998) Huntingtin acts in the nucleus to induce apoptosis but death does not correlate with the formation of intranuclear inclusions. Cell 95(1):55–66

12. Ravikumar B, Vacher C, Berger Z, Davies JE, Luo S, Oroz LG, Scaravilli F, Easton DF et al (2004) Inhibition of mTOR induces autophagy and reduces toxicity of polyglutamine expansions in fly and mouse models of Huntington disease. Nat Genet 36(6):585–595. https://doi.org/10.1038/ng1362
13. Annenkov A (2009) The insulin-like growth factor (IGF) receptor type 1 (IGF1R) as an essential component of the signalling network regulating neurogenesis. Mol Neurobiol 40(3):195–215. https://doi.org/10.1007/s12035-009-8081-0
14. Johnson-Farley NN, Travkina T, Cowen DS (2006) Cumulative activation of akt and consequent inhibition of glycogen synthase kinase-3 by brain-derived neurotrophic factor and insulin-like growth factor-1 in cultured hippocampal neurons. J Pharmacol Exp Ther 316(3):1062–1069. https://doi.org/10.1124/jpet.105.094433
15. Schechter R, Yanovitch T, Abboud M, Johnson G 3rd, Gaskins J (1998) Effects of brain endogenous insulin on neurofilament and MAPK in fetal rat neuron cell cultures. Brain Res 808(2):270–278
16. Moroo I, Yamada T, Makino H, Tooyama I, McGeer PL, McGeer EG, Hirayama K (1994) Loss of insulin receptor immunoreactivity from the substantia nigra pars compacta neurons in Parkinson's disease. Acta Neuropathol 87(4):343–348
17. Steen E, Terry BM, Rivera EJ, Cannon JL, Neely TR, Tavares R, Xu XJ, Wands JR et al (2005) Impaired insulin and insulin-like growth factor expression and signaling mechanisms in Alzheimer's disease—is this type 3 diabetes? J Alzheimers Dis 7(1):63–80
18. Parisi F, Riccardo S, Daniel M, Saqcena M, Kundu N, Pession A, Grifoni D, Stocker H et al (2011) Drosophila insulin and target of rapamycin (TOR) pathways regulate GSK3 beta activity to control Myc stability and determine Myc expression in vivo. BMC Biol 9:65. https://doi.org/10.1186/1741-7007-9-65
19. Singh MD, Raj K, Sarkar S (2014) Drosophila Myc, a novel modifier suppresses the poly(Q) toxicity by modulating the level of CREB binding protein and histone acetylation. Neurobiol Dis 63:48–61. https://doi.org/10.1016/j.nbd.2013.11.015
20. Bonini NM (1999) A genetic model for human polyglutamine-repeat disease in Drosophila melanogaster. Philos Trans R Soc Lond Ser B Biol Sci 354(1386):1057–1060. https://doi.org/10.1098/rstb.1999.0458
21. Warrick JM, Chan HY, Gray-Board GL, Chai Y, Paulson HL, Bonini NM (1999) Suppression of polyglutamine-mediated neurodegeneration in Drosophila by the molecular chaperone HSP70. Nat Genet 23(4):425–428. https://doi.org/10.1038/70532
22. Hay BA, Wolff T, Rubin GM (1994) Expression of baculovirus P35 prevents cell death in Drosophila. Development 120(8):2121–2129
23. Lin DM, Goodman CS (1994) Ectopic and increased expression of Fasciclin II alters motoneuron growth cone guidance. Neuron 13(3):507–523
24. Yang MY, Armstrong JD, Vilinsky I, Strausfeld NJ, Kaiser K (1995) Subdivision of the Drosophila mushroom bodies by enhancer-trap expression patterns. Neuron 15(1):45–54
25. Almudi I, Poernbacher I, Hafen E, Stocker H (2013) The Lnk/SH2B adaptor provides a fail-safe mechanism to establish the insulin receptor-Chico interaction. Cell Commun Signal 11(1):26. https://doi.org/10.1186/1478-811X-11-26
26. Weiss KR, Kimura Y, Lee WC, Littleton JT (2012) Huntingtin aggregation kinetics and their pathological role in a Drosophila Huntington's disease model. Genetics 190(2):581–600. https://doi.org/10.1534/genetics.111.133710
27. Steinert JR, Campesan S, Richards P, Kyriacou CP, Forsythe ID, Giorgini F (2012) Rab11 rescues synaptic dysfunction and behavioural deficits in a Drosophila model of Huntington's disease. Hum Mol Genet 21(13):2912–2922. https://doi.org/10.1093/hmg/dds117
28. Kumar JP, Jamal T, Doetsch A, Turner FR, Duffy JB (2004) CREB binding protein functions during successive stages of eye development in Drosophila. Genetics 168(2):877–893. https://doi.org/10.1534/genetics.104.029850
29. Chanu SI, Sarkar S (2016) Targeted downregulation of dMyc suppresses pathogenesis of human neuronal Tauopathies in Drosophila by limiting heterochromatin relaxation and tau hyperphosphorylation. Mol Neurobiol 54(4):2706–2719. https://doi.org/10.1007/s12035-016-9858-6
30. Lilja T, Qi D, Stabell M, Mannervik M (2003) The CBP coactivator functions both upstream and downstream of Dpp/screw signaling in the early Drosophila embryo. Dev Biol 262(2):294–302
31. Brand AH, Perrimon N (1993) Targeted gene expression as a means of altering cell fates and generating dominant phenotypes. Development 118(2):401–415
32. Chan HY, Warrick JM, Andriola I, Merry D, Bonini NM (2002) Genetic modulation of polyglutamine toxicity by protein conjugation pathways in Drosophila. Hum Mol Genet 11(23):2895–2904
33. Hay BA, Wassarman DA, Rubin GM (1995) Drosophila homologs of baculovirus inhibitor of apoptosis proteins function to block cell death. Cell 83(7):1253–1262
34. Branco J, Al-Ramahi I, Ukani L, Perez AM, Fernandez-Funez P, Rincon-Limas D, Botas J (2008) Comparative analysis of genetic modifiers in Drosophila points to common and distinct mechanisms of pathogenesis among polyglutamine diseases. Hum Mol Genet 17(3):376–390. https://doi.org/10.1093/hmg/ddm315
35. Guo L, Giasson BI, Glavis-Bloom A, Brewer MD, Shorter J, Gitler AD, Yang X (2014) A cellular system that degrades misfolded proteins and protects against neurodegeneration. Mol Cell 55(1):15–30. https://doi.org/10.1016/j.molcel.2014.04.030
36. Quinn WG, Harris WA, Benzer S (1974) Conditioned behavior in Drosophila melanogaster. Proc Natl Acad Sci U S A 71(3):708–712
37. Cohen-Carmon D, Meshorer E (2012) Polyglutamine (polyQ) disorders: the chromatin connection. Nucleus 3(5):433–441. https://doi.org/10.4161/nucl.21481
38. Fahrbach SE (2006) Structure of the mushroom bodies of the insect brain. Annu Rev Entomol 51:209–232. https://doi.org/10.1146/annurev.ento.51.110104.150954
39. Kurusu M, Awasaki T, Masuda-Nakagawa LM, Kawauchi H, Ito K, Furukubo-Tokunaga K (2002) Embryonic and larval development of the Drosophila mushroom bodies: concentric layer subdivisions and the role of fasciclin II. Development 129(2):409–419
40. Chou AH, Yeh TH, Kuo YL, Kao YC, Jou MJ, Hsu CY, Tsai SR, Kakizuka A et al (2006) Polyglutamine-expanded ataxin-3 activates mitochondrial apoptotic pathway by upregulating Bax and downregulating Bcl-xL. Neurobiol Dis 21(2):333–345. https://doi.org/10.1016/j.nbd.2005.07.011
41. Meier P, Silke J, Leevers SJ, Evan GI (2000) The Drosophila caspase DRONC is regulated by DIAP1. EMBO J 19(4):598–611. https://doi.org/10.1093/emboj/19.4.598
42. Chen M, Ona VO, Li M, Ferrante RJ, Fink KB, Zhu S, Bian J, Guo L et al (2000) Minocycline inhibits caspase-1 and caspase-3 expression and delays mortality in a transgenic mouse model of Huntington disease. Nat Med 6(7):797–801. https://doi.org/10.1038/77528
43. Kasten FH (1967) Cytochemical studies with acridine orange and the influence of dye contaminants in the staining of nucleic acids. Int Rev Cytol 21:141–202
44. Fan Y, Bergmann A (2010) The cleaved-Caspase-3 antibody is a marker of Caspase-9-like DRONC activity in Drosophila. Cell Death Differ 17(3):534–539. https://doi.org/10.1038/cdd.2009.185
45. Chai Y, Koppenhafer SL, Bonini NM, Paulson HL (1999) Analysis of the role of heat shock protein (Hsp) molecular chaperones in polyglutamine disease. J Neurosci 19(23):10338–10347
46. Velazquez JM, Sonoda S, Bugaisky G, Lindquist S (1983) Is the major Drosophila heat shock protein present in cells that have not been heat shocked? J Cell Biol 96(1):286–290

47. Strzyz P (2017) Mechanisms of diseases: Excessive polyQ tracts curb autophagy. Nat Rev Mol Cell Biol 18(6):344. https://doi.org/10.1038/nrm.2017.50
48. Wong E, Cuervo AM (2010) Autophagy gone awry in neurodegenerative diseases. Nat Neurosci 13(7):805–811. https://doi.org/10.1038/nn.2575
49. Krench M, Littleton JT (2017) Neurotoxicity pathways in Drosophila models of the polyglutamine disorders. Curr Top Dev Biol 121:201–223. https://doi.org/10.1016/bs.ctdb.2016.07.006
50. Labbadia J, Morimoto RI (2015) The biology of proteostasis in aging and disease. Annu Rev Biochem 84:435–464. https://doi.org/10.1146/annurev-biochem-060614-033955
51. Kroemer G, Marino G, Levine B (2010) Autophagy and the integrated stress response. Mol Cell 40(2):280–293. https://doi.org/10.1016/j.molcel.2010.09.023
52. Hara T, Nakamura K, Matsui M, Yamamoto A, Nakahara Y, Suzuki-Migishima R, Yokoyama M, Mishima K et al (2006) Suppression of basal autophagy in neural cells causes neurodegenerative disease in mice. Nature 441(7095):885–889. https://doi.org/10.1038/nature04724
53. Komatsu M, Waguri S, Chiba T, Murata S, Iwata J, Tanida I, Ueno T, Koike M et al (2006) Loss of autophagy in the central nervous system causes neurodegeneration in mice. Nature 441(7095):880–884. https://doi.org/10.1038/nature04723
54. Rubinsztein DC, Gestwicki JE, Murphy LO, Klionsky DJ (2007) Potential therapeutic applications of autophagy. Nat Rev Drug Discov 6(4):304–312. https://doi.org/10.1038/nrd2272
55. Mizushima N, Levine B, Cuervo AM, Klionsky DJ (2008) Autophagy fights disease through cellular self-digestion. Nature 451(7182):1069–1075. https://doi.org/10.1038/nature06639
56. Yamamoto A, Cremona ML, Rothman JE (2006) Autophagy-mediated clearance of huntingtin aggregates triggered by the insulin-signaling pathway. J Cell Biol 172(5):719–731. https://doi.org/10.1083/jcb.200510065
57. DeVorkin L, Gorski SM (2014) LysoTracker staining to aid in monitoring autophagy in Drosophila. Cold Spring Harb Protoc 2014(9):951–958. https://doi.org/10.1101/pdb.prot080325
58. Wu J, Dang Y, Su W, Liu C, Ma H, Shan Y, Pei Y, Wan B et al (2006) Molecular cloning and characterization of rat LC3A and LC3B—two novel markers of autophagosome. Biochem Biophys Res Commun 339(1):437–442. https://doi.org/10.1016/j.bbrc.2005.10.211
59. Kabeya Y, Mizushima N, Ueno T, Yamamoto A, Kirisako T, Noda T, Kominami E, Ohsumi Y et al (2000) LC3, a mammalian homologue of yeast Apg8p, is localized in autophagosome membranes after processing. EMBO J 19(21):5720–5728. https://doi.org/10.1093/emboj/19.21.5720
60. Tanida I, Ueno T, Kominami E (2008) LC3 and autophagy. Methods Mol Biol 445:77–88. https://doi.org/10.1007/978-1-59745-157-4_4
61. Schmidt T, Landwehrmeyer GB, Schmitt I, Trottier Y, Auburger G, Laccone F, Klockgether T, Volpel M et al (1998) An isoform of ataxin-3 accumulates in the nucleus of neuronal cells in affected brain regions of SCA3 patients. Brain Pathol 8(4):669–679
62. Paulson HL, Perez MK, Trottier Y, Trojanowski JQ, Subramony SH, Das SS, Vig P, Mandel JL et al (1997) Intranuclear inclusions of expanded polyglutamine protein in spinocerebellar ataxia type 3. Neuron 19(2):333–344
63. Ye L, Maji S, Sanghera N, Gopalasingam P, Gorbunov E, Tarasov S, Epstein O, Klein-Seetharaman J (2017) Structure and dynamics of the insulin receptor: implications for receptor activation and drug discovery. Drug Discov Today 22:1092–1102. https://doi.org/10.1016/j.drudis.2017.04.011
64. Hamelers IH, Steenbergh PH (2003) Interactions between estrogen and insulin-like growth factor signaling pathways in human breast tumor cells. Endocr Relat Cancer 10(2):331–345
65. Mester J, Redeuilh G (2008) Proliferation of breast cancer cells: regulation, mediators, targets for therapy. Anti Cancer Agents Med Chem 8(8):872–885
66. Coelho CM, Leevers SJ (2000) Do growth and cell division rates determine cell size in multicellular organisms? J Cell Sci 113(Pt 17):2927–2934
67. Edgar BA (2006) How flies get their size: genetics meets physiology. Nat Rev Genet 7(12):907–916. https://doi.org/10.1038/nrg1989
68. Konishi T, Takeyasu A, Natsume T, Furusawa Y, Hieda K (2011) Visualization of heavy ion tracks by labeling 3'-OH termini of induced DNA strand breaks. J Radiat Res 52(4):433–440
69. Escudero LM, Freeman M (2007) Mechanism of G1 arrest in the Drosophila eye imaginal disc. BMC Dev Biol 7(13):13. https://doi.org/10.1186/1471-213X-7-13
70. Yamaguchi M, Hirose F, Inoue YH, Shiraki M, Hayashi Y, Nishi Y, Matsukage A (1999) Ectopic expression of human p53 inhibits entry into S phase and induces apoptosis in the Drosophila eye imaginal disc. Oncogene 18(48):6767–6775. https://doi.org/10.1038/sj.onc.1203113
71. McCampbell A, Taylor JP, Taye AA, Robitschek J, Li M, Walcott J, Merry D, Chai Y et al (2000) CREB-binding protein sequestration by expanded polyglutamine. Hum Mol Genet 9(14):2197–2202
72. Nucifora FC Jr, Sasaki M, Peters MF, Huang H, Cooper JK, Yamada M, Takahashi H, Tsuji S et al (2001) Interference by huntingtin and atrophin-1 with cbp-mediated transcription leading to cellular toxicity. Science 291(5512):2423–2428. https://doi.org/10.1126/science.1056784
73. Ludlam WH, Taylor MH, Tanner KG, Denu JM, Goodman RH, Smolik SM (2002) The acetyltransferase activity of CBP is required for wingless activation and H4 acetylation in Drosophila melanogaster. Mol Cell Biol 22(11):3832–3841
74. Puig O, Tjian R (2005) Transcriptional feedback control of insulin receptor by dFOXO/FOXO1. Genes Dev 19(20):2435–2446. https://doi.org/10.1101/gad.1340505
75. Sakamoto K, Iwasaki K, Sugiyama H, Tsuji Y (2009) Role of the tumor suppressor PTEN in antioxidant responsive element-mediated transcription and associated histone modifications. Mol Biol Cell 20(6):1606–1617. https://doi.org/10.1091/mbc.E08-07-0762
76. Chen YL, Law PY, Loh HH (2008) NGF/PI3K signaling-mediated epigenetic regulation of delta opioid receptor gene expression. Biochem Biophys Res Commun 368(3):755–760. https://doi.org/10.1016/j.bbrc.2008.01.164
77. Wyss-Coray T (2016) Ageing, neurodegeneration and brain rejuvenation. Nature 539(7628):180–186. https://doi.org/10.1038/nature20411
78. Fernandez R, Tabarini D, Azpiazu N, Frasch M, Schlessinger J (1995) The Drosophila insulin receptor homolog: a gene essential for embryonic development encodes two receptor isoforms with different signaling potential. EMBO J 14(14):3373–3384
79. White MF, Kahn CR (1994) The insulin signaling system. J Biol Chem 269(1):1–4
80. Li CR, Guo D, Pick L (2013) Independent signaling by Drosophila insulin receptor for axon guidance and growth. Front Physiol 4:385. https://doi.org/10.3389/fphys.2013.00385
81. Reis SD, Pinho BR, Oliveira JM (2016) Modulation of molecular chaperones in Huntington's disease and other polyglutamine disorders. Mol Neurobiol 54:5829–5854. https://doi.org/10.1007/s12035-016-0120-z
82. Kaur J, Debnath J (2015) Autophagy at the crossroads of catabolism and anabolism. Nat Rev Mol Cell Biol 16(8):461–472. https://doi.org/10.1038/nrm4024
83. Hyttinen JM, Amadio M, Viiri J, Pascale A, Salminen A, Kaarniranta K (2014) Clearance of misfolded and aggregated proteins by aggrephagy and implications for aggregation

diseases. Ageing Res Rev 18:16–28. https://doi.org/10.1016/j.arr.2014.07.002

84. Lamark T, Johansen T (2012) Aggrephagy: selective disposal of protein aggregates by macroautophagy. Int J Cell Biol 2012: 736905. https://doi.org/10.1155/2012/736905
85. Yang H, Hu HY (2016) Sequestration of cellular interacting partners by protein aggregates: implication in a loss-of-function pathology. FEBS J 283(20):3705–3717. https://doi.org/10.1111/febs.13722
86. Ogryzko VV, Schiltz RL, Russanova V, Howard BH, Nakatani Y (1996) The transcriptional coactivators p300 and CBP are histone acetyltransferases. Cell 87(5):953–959